Electrochemical approaches based on micro- and nanomaterials for diagnosing oxidative stress

Mahdi Jamshidi, Alain Walcarius, Madasamy Thangamuthu, Masoud Mehrgardi, Akram Ranjbar

▶ **To cite this version:**

Mahdi Jamshidi, Alain Walcarius, Madasamy Thangamuthu, Masoud Mehrgardi, Akram Ranjbar. Electrochemical approaches based on micro- and nanomaterials for diagnosing oxidative stress. Microchimica Acta, 2023, 190 (4), pp.117. 10.1007/s00604-023-05681-7 . hal-04262777

HAL Id: hal-04262777
https://hal.univ-lorraine.fr/hal-04262777v1

Submitted on 27 Oct 2023

HAL is a multi-disciplinary open access archive for the deposit and dissemination of scientific research documents, whether they are published or not. The documents may come from teaching and research institutions in France or abroad, or from public or private research centers.

L'archive ouverte pluridisciplinaire **HAL**, est destinée au dépôt et à la diffusion de documents scientifiques de niveau recherche, publiés ou non, émanant des établissements d'enseignement et de recherche français ou étrangers, des laboratoires publics ou privés.

Electrochemical approaches based on micro and nanomaterials for diagnosing oxidative stress

Mahdi Jamshidi[1,2*], Alain Walcarius[3], Madasamy Thangamuthu[4*], Masoud Mehrgardi[5], Akram Ranjbar[1,2]*

[1] Department of Toxicology and Pharmacology, School of Pharmacy, Hamadan University of Medical Sciences, Hamadan, Iran. (Akranjbar2015@gmail.com, Dehnavi.m293@gmail.com)

[2] Nutrition Health Research Center, Hamadan University of Medical Sciences, Hamadan, Iran

[3] Laboratory of Physical Chemistry and Microbiology for Materials and the Environment, Université de Lorraine, CNRS, LCPME, Nancy, France.

[4] Department of Chemical Engineering, University College London, Torrington Place, WC1E 7JE, United Kingdom. (m.thangamuthu@ucl.ac.uk)

[5] Department of Chemistry, University of Isfahan, Isfahan 81746-73441, Iran.

*Corresponding Authors (Akranjbar2015@gmail.com)

These authors contributed equally to this work.

Abstract

This review article comprehensively discusses the various electrochemical approaches for measuring and detecting oxidative stress biomarkers and enzymes, particularly reactive oxygen/ nitrogen species, highly reactive chemical molecules, which are the byproducts of normal aerobic metabolism and can oxidize cellular components such as DNA, lipids, and proteins. First, we address the latest research on the electrochemical determination of reactive oxygen species generating enzymes, followed by detection of oxidative stress biomarkers, and final determination of total antioxidant activity (endogenous and exogenous). Most electrochemical sensing platforms exploited the unique properties of micro and nanomaterials such as carbon nanomaterials, metal or metal oxide nanoparticles (NPs), conductive polymers and metal-nano compounds, which have been mainly used for enhancing the electrocatalytic response of sensors/biosensors. The performance of the electroanalytical device commonly measured by cyclic voltammetry (CV) and differential pulse voltammetry (DPV) in terms of detection limit, sensitivity, and linear range of detection was also discussed. This article provides a comprehensive review of electrode fabrication, characterization and evaluation of their performances, which are assisting to design and manufacture an appropriate electrochemical (bio)sensor for medical and clinical applications. The key points such as accessibility, affordability, rapidity, low cost, and high sensitivity of the electrochemical sensing devices were also highlighted for the diagnosis of oxidative stress. Overall, this review brings a timely discussion on past and current approaches for developing electrochemical sensors and biosensors mainly based on micro and nanomaterials for the diagnosis of oxidative stress.

Keywords

Electrochemical sensor and biosensor, Micro and nanomaterials, Oxidative stress, Biomarkers, Exogenous and endogenous antioxidants, Reactive oxygen species.

Table of content

1. Introduction

The set of *in vivo* aerobic activities of enzymes and metabolic reactions (mitochondrial electron transfer cycles) causes the production or consumption of reactive oxygen/nitrogen species (ROS/RNS) such as hydroxyl radicals, peroxynitrite, and hydrogen peroxide [1]. These are formed in peroxisomes, cytochrome P450, mitochondria, and other cellular constituent components [2]. In a healthy and ideal status, there is an acceptable balance between these species and the body's antioxidant system. However, high activity of ROS/RNS generation enzymes, destructive environmental factors (ultraviolet/infrared radiation, poisoning with organophosphorus, stressors, air pollutants, cigarette smoking, low consumption of food containing antioxidants), and low efficiency of antioxidant enzymes lead to oxidative or nitrosative stress [3,4]. The main victims of these biological processes are macromolecules (DNA, proteins, lipids), and their biochemical variations cause the promotion of some disorders and diseases such as aging, Parkinson's, Alzheimer's, diabetes mellitus, obesity, acute poisoning, etc. [5]. This pathological or physiological process generates certain electroactive molecules known as biomarkers via hydroxylation, nitration [6], oxidative deamination (reactive carbonyl moiety) [7], and free radical chain oxidation (O_2 addition to carbon radicals; fragmentation of peroxyl radical) [8] reactions. Oxidative stress can be diagnosed by monitoring oxidation adducts of DNA, proteins, lipids, the activity of enzymes, and antioxidants status [9,10] (Scheme 1). Several methodological approaches such as luminescence [11], electron spin resonance [12], colorimetric [13], chemiluminescence [14], liquid chromatography-tandem mass spectroscopy [15], fluorescence [16], and surface-enhanced Raman spectroscopy [17] have been reported so far for detecting the oxidative stress biomarkers. These detection techniques are limited due to the requirement of more sophisticated equipment, expensive facilities, involve pretreatment steps

such as solid-phase extraction, time-consuming and labeling processes. Unlike these techniques, the electrochemical sensing approach accompanied with nanotechnology offers a variety of outstanding features, for example, instrumental simplicity, fast, moderate operational cost, high sensitivity and specificity, and have potential for portability and miniaturization. Various kinds of nanosystems based on metallic (metal organic frameworks, magnetic NPs, metal oxides) carbon (nanotubes, graphenes, Quantum dots), and biological (antibody, aptamer) nanomaterials are being gradually applied to electrochemical sensor and biosensors because of their incomparable physical, magnetic, chemical, and mechanical properties. The lifetime and the half-wave potential of the redox couple of biomarkers are crucial factors to detect oxidative stress biomarkers in biological conditions using electrochemical methods [18-20]. Activity retention of the labile biomolecules and reusability of a biosensor are two crucial parameters as the commercial viability of a device. Therefore, decreasing of inactivation mechanisms of biomaterials (proteins and enzymes) such as unfolding, poisoning, proteolysis, lose of Co-factor, chemistry of macromolecule changing, and protein aggregation could be effective for enhancing of the storage and operational lifetime. The electrochemical signal corresponding to the concentration of the analytes can be obtained using potential step (differential pulse voltammetry, normal pulse voltammetry, chronoamperometry and etc.) and sweep (cyclic voltammetry and linear sweep voltammetry) methods [21,22] (Scheme 2).

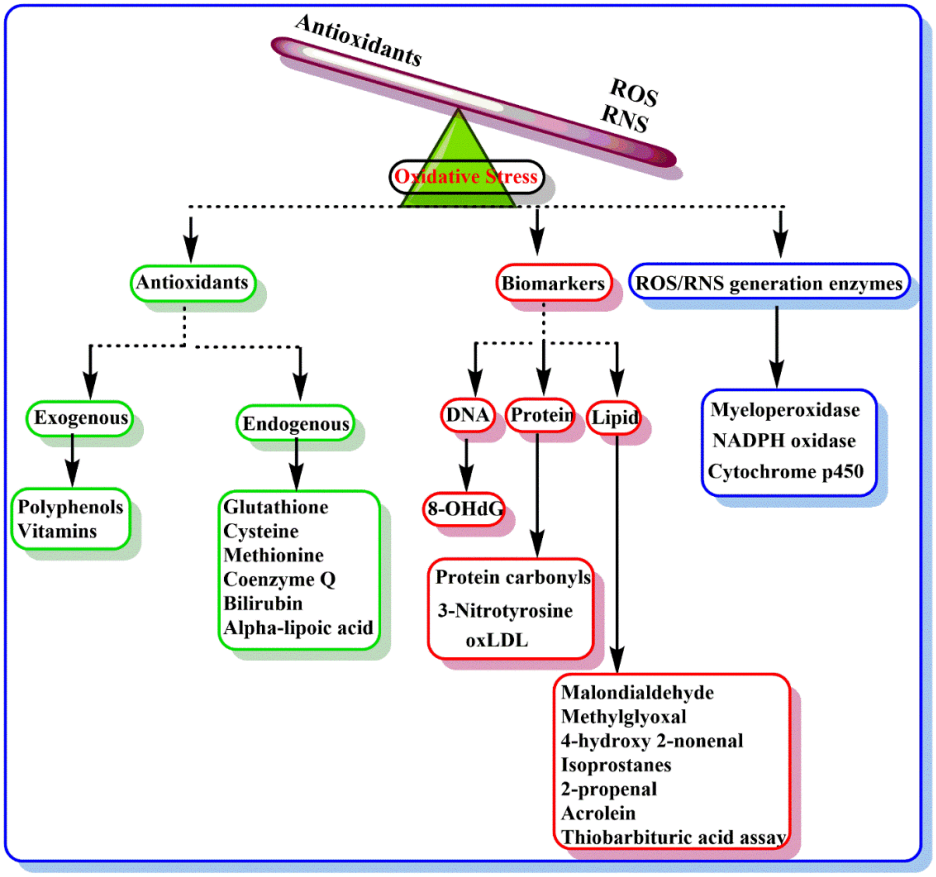

Scheme 1. Overview of antioxidants, biomarkers, and enzymes for investigation of oxidative stress status.

In this review, a comprehensive study is provided for the electrochemical determination of ROS/RNS generation enzymes, biomarkers, and antioxidants. Overall, it is comprised of several main sections. The first one described the electrochemical determination of ROS enzymes such as Myeloperoxidase, NADPH oxidase, and Cytochrome P450. Several designs of biosensing electrodes were discussed and compared their activities towards the determination of oxidative stress enzymes. Development of a wide spectrum of recognition elements based on nanomaterials, metal-nanoparticles, conductive polymers, and bio-elements (enzymes, antibodies, aptamers, DNA) [23] was discussed. The next sections were dealing with the electrochemical detection of biomarkers of the oxidative stress. The several competitive approaches for the detection of oxidative protein damage biomarkers such as protein carbonyls, 3-nitrotyrosine, and oxidized low-density lipoprotein (oXLDL) were first discussed, especially with respect to the advantage of electrochemical sensing techniques. Then, the electrochemical detection of oxidative lipid damage biomarkers was described in detail that the essential biomarkers such as Malondialdehyde, Methylglyoxal, 4-hydroxy 2-nonenal (HNE), 2-Propenal (Acrolein), 8-isoprostane and F2-isoprostanes, and Thiobarbituric acid-reactive substances (TBARS) biological generation and their significance to biomedical and clinical research were also discussed. In addition, pictorial representation of the protein's oxidation process was shown to easily understand the readers. In the same section, we also discussed the reports on electrochemical detection of oxidative DNA damage biomarkers, especially 8-hydroxy-deoxyguanosine (8-OHdG). Electrochemical determination of endogenous antioxidants such as Glutathione (reduced GSH/ oxidized GSSG), cysteine, methionine, coenzyme Q, α-lipoic acid, and bilirubin were discussed in the final sections. The detailed sketch of the electrochemical research on developing sensors/biosensors for oxidative stress biomarkers and the challenging facts addressed to attain commercial electrochemical assay kits in this review would assist future researchers in biomedical research to understand the state-of-the-art electrochemical approaches for diagnosing oxidative stress and provoke to design an affordable electrochemical device for monitoring one or more biomarkers in one go.

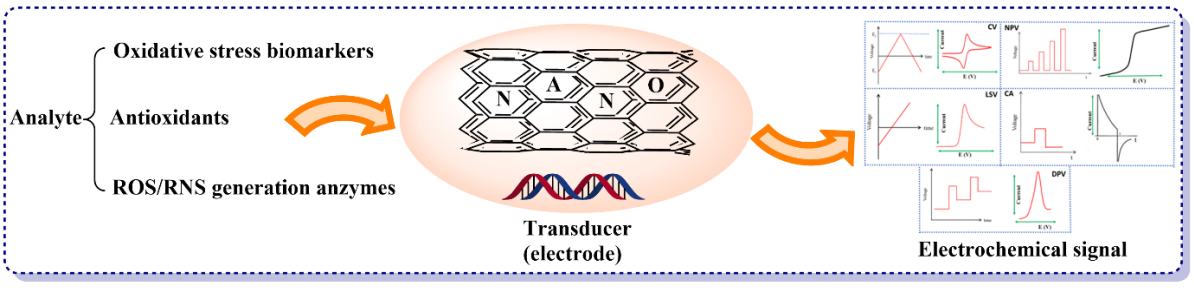

Scheme. 2 Schematic representation of the working principle of the electrochemical

techniques used for detection and diagnosis of oxidative stress.

2. Electrochemical determination of ROS generation enzymes

2.1. Myeloperoxidase

Myeloperoxidase (MPO), a protein with a heme core, is available in azurophilic granules, macrophages, and neutrophils. The most important reaction catalyzed by MPO is the production of Hypochlorous acid (HOCl) in the presence of chloride and hydrogen peroxide [24]. HOCl, a potent oxidizing agent, can modify biomolecules such as DNA, proteins, and lipids by chlorinating and oxidizing processes followed by a series of enzymatic and non-enzymatic cascade reactions in the body's biological system. The results of these reactions are either products with oxidizing properties or reactive intermediates such as ROS and RNS [25]. These products originating from MPO activity (at least initially) can be involved in a broad spectrum of reactions such as oxidation, peroxidation, nitration, chlorination, carbamylation, nitrosylation and thus change the structure and function of important macromolecules (DNA, lipids, or proteins) [26, 27]. To better understand the activities of MPO, several investigations have been made (notably based on different oxidation states of Fe centers) to elucidate the possible catalytic mechanisms operating in the biological system. Recently, Ndrepepa [28] reported a complete set of MPO processes and functions in the biological system and explained the association between MPO activity, oxidative stress, and cardiovascular disease. As seen in Fig. 1. several different sources such as xanthine oxidase, nitric oxide synthase (NOS), superoxide dismutase (SOD), and nicotinamide adenine dinucleotide phosphate oxidase (NADPH oxidase) are available to generate H_2O_2 to initiate the MPO catalytic cycle reaction followed by several MPO reactions can take place depending on the species-environment.

Thus, there is a direct correlation between oxidative stress and the increasing activity of the MPO enzyme. For instance, cardiovascular [29], and fibrotic [30], are related to increasing MPO levels. Hence, MPO has been considered as an important biomarker for diagnosing oxidative stress-related disorders, and its determination in blood serum is essential. Electrochemical biosensors (EB) have been widely used for detecting MPO, more specifically, immunosensors, which are prepared by immobilizing the antibody of MPO (anti-MPO) onto a modified electrode surface, for selective recognition of MPO in solution. Liu and Lu [31] constructed electrochemical immunosensors using the sandwich model to assess MPO concentration in serum samples. The stepwise fabrication of this immunosensor is illustrated in Fig. 2. Briefly, the glassy carbon (GC) electrode was first modified with gold nanoparticles (AuNP) and graphene oxide (GO) to increase the surface area and conductivity. Then, the MPO capture antibody was coated on GC/AuNP-GO electrode to determine MPO. To complement the other side of the sandwich model, they encapsulated the gold nanoparticles in graphitized mesoporous carbons

(AuNP@GMC) to immobilize horseradish peroxidase (HRP)-labeled antibody (HRP@Ab2). The MPO concentration in serum samples was monitored by measuring the electrochemical reduction of H_2O_2 using the amperometry technique at a constant potential of −0.18 V vs. Ag/AgCl. The linear range and detection limit were reported as 1-300 and 0.1 pg/mL, respectively. The sensor response was kept after one month storage at 4°C.

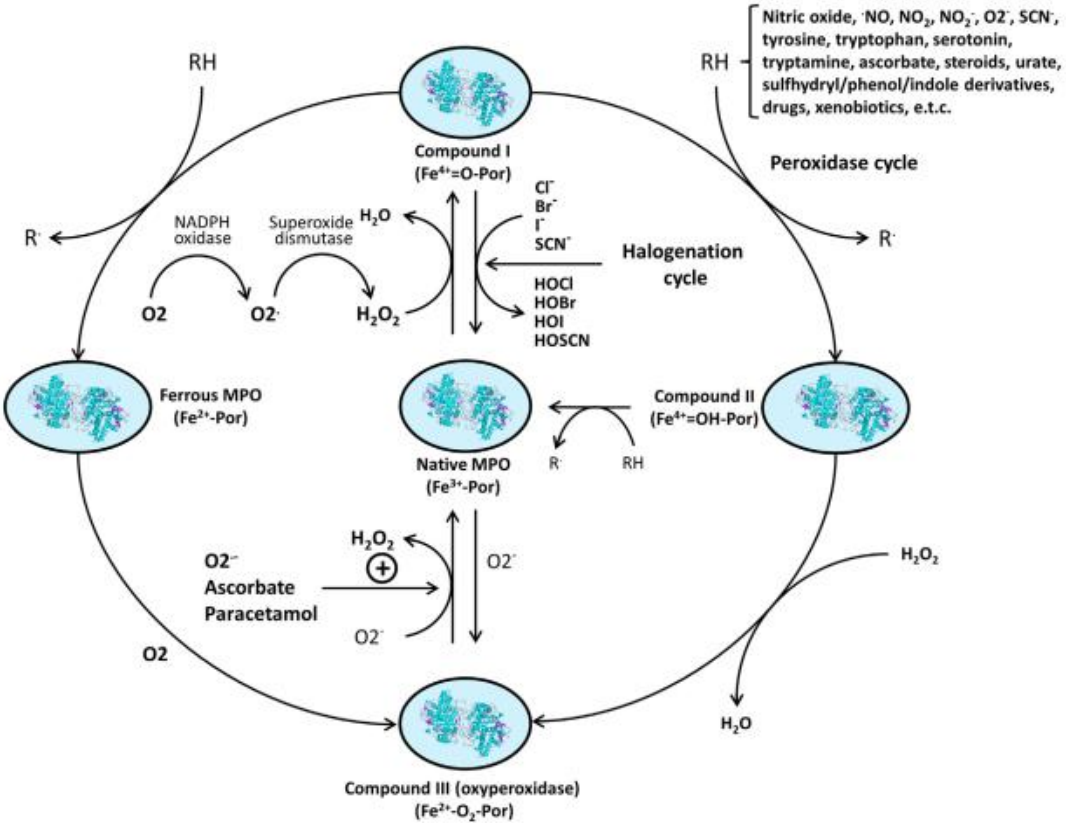

Fig. 1 The set of reactions catalyzed by the MPO enzyme [28].

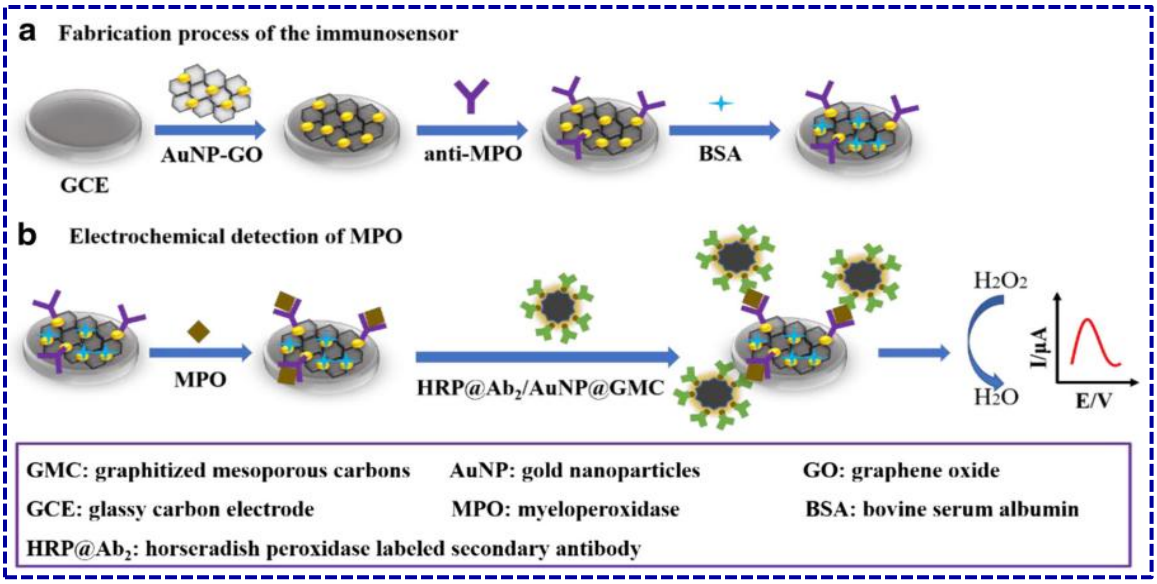

Fig. 2 Electrochemical immunosensor for determination of MPO [31].

In another immunoassay strategy, Bekhit and Gorski [32] detected MPO by monitoring of H_2O_2 consumption reaction in two systems, i) the reaction of MPO in the presence of H_2O_2 and thiocyanate ion (SCN^-), and ii) the reduction of H_2O_2 with a catalase-like system on nitrogen-doped carbon nanotubes (N-CNT) electrode (Fig. 3). This amperometric biosensor detected 5.2 μg L^{-1} of MPO in human saliva.

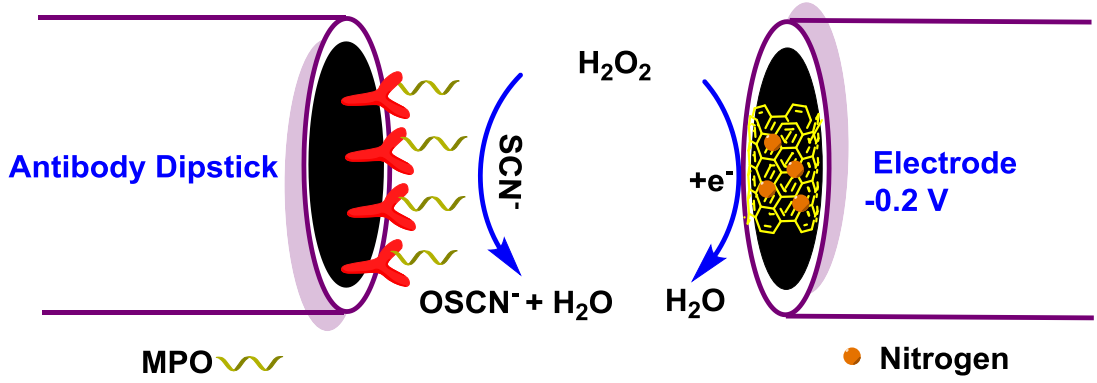

Fig. 3 Two electrochemical strategies base on H_2O_2 reduction for measurement of MPO level [32].

The various composite films have been reported for the electrochemical determination of MPO levels in biological samples. Some sensors for the detection of MPO using such composite films [33-35] were shown in Table 1 (see Table S1 in SI for a more comprehensive view) and compared their electroanalytical performances in terms of detection limit, and linear range of

concentration. The utilization of nanomaterials offers excellent biocompatibility, conductive properties, high surface-to-volume ratio, high mechanical strength, and rapid functionalization to increase the analytical feature of MPO detection.

Table 1. Examples of modified electrodes with analytical parameters for the detection of MPO.

Modified electrode	**LOD (µg/mL)**	**Linear range (µg/mL)**	**Method**	**Reference**
Magnetic Switch Au/SPE/Pt	0.0004	0.0009-0.06	CA	[33]
MWCNTs/THI/GNPs/CHIT/anti-MPO/GCE	1.425	2.5-125	CV	[34]
anti-MPO/nanogold/nanoCeO_2-$BMIMPF_6$/l-Cysteine/Au	0.06	10.0-400	CV	[35]

SPE: screen-printed electrode, MWCNTs: multiwall carbon nanotubes, THI/GNPs/CHIT: Thionine/Gold Nanoparticles-Chitosan, GCE: glassy carbon electrode, $BMIMPF_6$: 1-butyl-3-methylimidazolium hexafluorophosphate, CA: Chronoamperometry, CV: Cyclic voltammetry.

2.2. NADPH oxidase

NADPH oxidases (nicotinamide adenine dinucleotide phosphate oxidase), reductive enzymes, are one of the most important sources of ROS production. The family of NADPH oxidase (NOX) has been classified from seven isomers and subunits (NOX1-5 and dual oxidases 1 and 2 (DUOX1-2)) in the human body [36]. These enzymes are found in the cell membrane and most of them catalyze the reaction of producing superoxide ions from oxygen (electron acceptor) during the oxidation-reduction process, and simultaneously NADPH (electron donor) is oxidized to $NADP^+$ [37]. Drummond and their coworkers reported the direct relationship between the increased activity of NADPH oxidase level, and ROS generation, oxidative stress, vascular disease, and stroke [38]. Fig. 4 shows a cross-section of an artery that indicates the presence of each NADPH enzyme at different levels of the blood vessel wall. The reactions catalyzed with NOX1, NOX2, NOX4, and NOX5 enzymes are also shown in different parts, in addition to the superoxide anion radical.

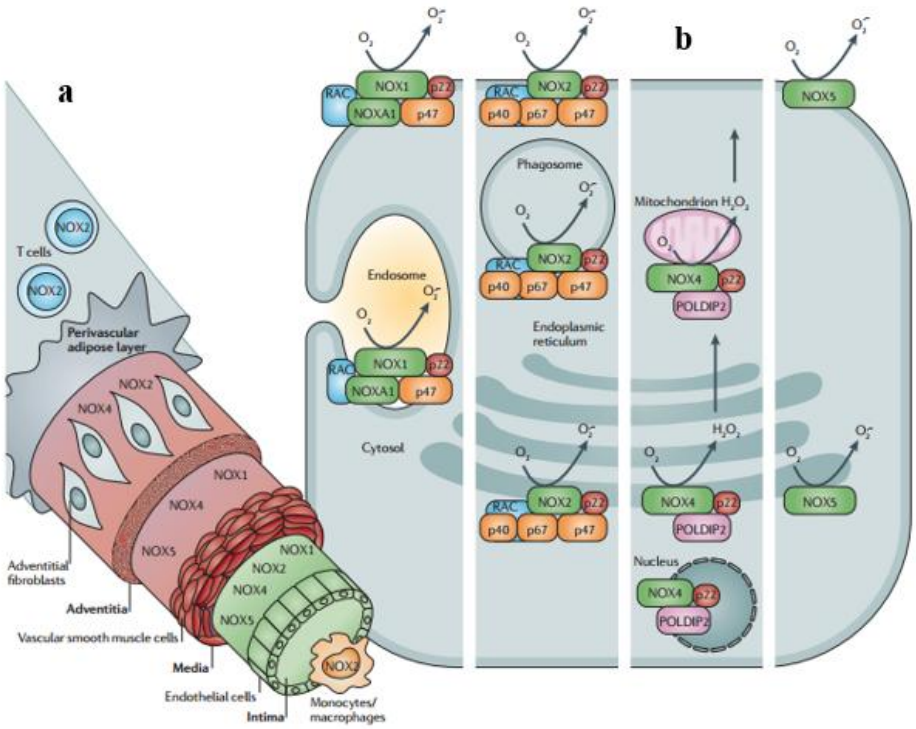

Fig. 4 Cellular and subcellular expression of NADPH oxidase isoforms in the blood vessel wall. a) Schematic diagram showing cellular localization (endothelial cells, vascular smooth muscle cells, fibroblasts, macrophages and T cells) of NADPH oxidase isoforms (NOX1 oxidase, NOX2 oxidase, NOX4 oxidase and NOX5 oxidase) through a cross-section of an artery. **b)** Schematic diagram of a hypothetical cell in which all of the vascular NADPH oxidase isoforms (starting with NOX1 oxidase in the left hand column and finishing with NOX5 oxidase in the right hand column) are expressed in each of their possible subcellular locations [38].

The increasing NADPH oxidase activity can be observed during the vascular, cardiovascular, coronary artery diseases, and neurodegenerative disorders (Alzheimer's, Parkinson's, Huntington's diseases) [39], and hence the determination of NOX level is extremely essential. Electrochemical approaches have been proposed for the determination of NOX in biological samples due to the excellent sensitivity and high stability at a low cost. Sekioka et al. developed an electrochemical GABA (γ-aminobutyric acid) sensor on electron cyclotron resonance (ECR)-bovine serum albumin-carbon film electrode (ECR/BSA/CE) to detect NOX in solution [40]. The detection limit of the modified electrode (10 nM) was about 25 times less than the bare electrode (250 nM), with better resistance to fouling than GCE. Ashkenazi and coworkers detected the NOX activity in human neutrophils and DMSO-induced PLB 985 cells using chemiluminescence and amperometric methods [41]. Isoluminol was used as a chemiluminescence (CL) substrate to produce the light corresponding to the concentration of NOx, which is dependent on superoxide activity. In the amperometric detection, NOX activity is

determined using the oxidation of H_2O_2 at +0.65 V (Fig. 5). Though both methods were highly sensitive and show fast response, the electrochemical process does not require any additive to measure NOX. The detection limits for amperometry and CL procedures are 17 ± 6 and 8 ± 2 µM, respectively.

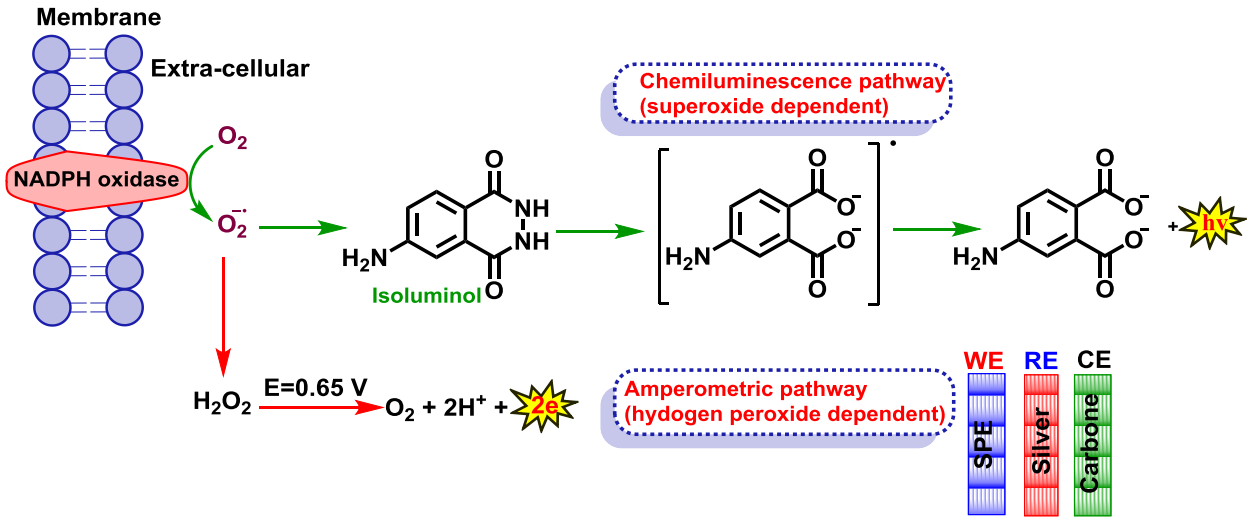

Fig. 5 Experimental design of extracellular superoxide and hydrogen peroxide detection by the isoluminol CL and electrochemical techniques [41].

2.3 Cytochrome P450

Cytochromes P450 (CYP), a heme-containing enzyme, can have both positive and negative effects on the metabolism of the human body's biological system. The positive effect of CYP is its ability to metabolize a wide range of foreign compounds such as hydrocarbons, drugs, xenobiotics, and carcinogens. Such a metabolic process implies the addition of an oxygen atom to non-polar compounds, leading to their conversion into relatively polar compounds via the monooxygenase catalytic cycle. This process has occurred more in the liver and can lead to the repulse of harmful substances through the kidneys [42].

As noted earlier, there is a direct relationship between cytochrome P450 activity and ROS level. Also, the metabolic cycle of drugs is associated with inhibition or activation of the CYPs enzyme. Therefore, two electrochemical approaches were reported to measure CYP450 enzymes: direct and indirect (determination of organic compounds (RH) level) assessment of oxidative stress status. Direct electrochemical reduction or oxidation of CYP450 enzyme has been carried out on various electrode surfaces [43]. For example, Fantuzzi and et al. investigated the electrochemical behavior of the P450 2E1 enzyme on gold (Au) and glassy carbon (GC) electrodes in 298K [44]. The cyclic voltammetry results reveal the existence of a redox couple (Fe^{III}/Fe^{II}) originating from the P450 2E1 enzyme, which is either covalently or physically adsorbed onto the electrode surface. Sodium montmorillonite, zirconium dioxide nanoparticles [45], didodecyldimethylammonium bromide (DDAB) [43,46], modified electrodes were reported

for studying electron transfer process of various CYP450 enzymes [47]. The catalytic cycle of cytochrome P450 has been largely exploited for electrochemical detection in a wide range of drugs such as naproxen [48], caffeine [49], cocaine, cyclophosphamide, ifosfamide, ftorafur, etoposide, and aflatoxin B1 in biological samples. Real-time delivery of naproxen was successfully achieved by cyclic voltammetry over a period of 16 hours [48]. Hence it has generated tremendous pharmaceutical applications and sensor manufacturing with high sensitivity and selectivity. For a better perception, a general scheme of cytochrome sensors is shown in Fig. 6.

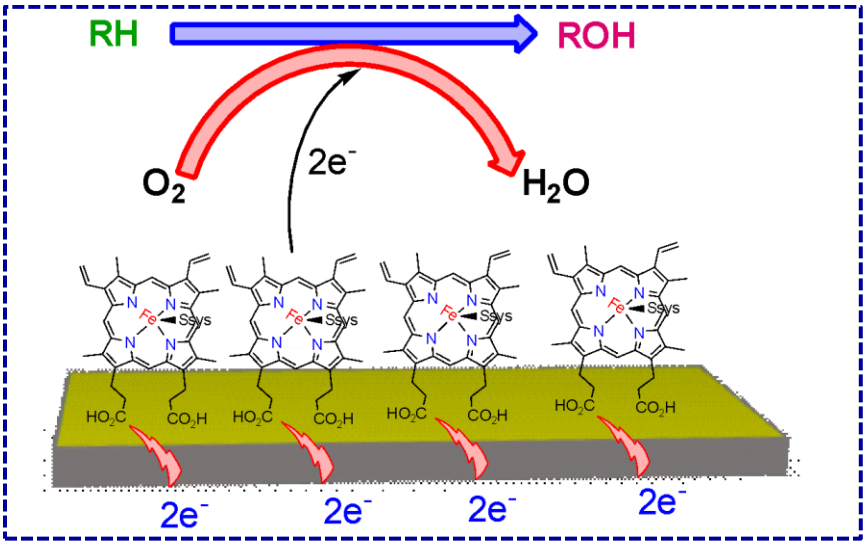

Fig. 6 Schematic representation of CYP sensor.

3. Electrochemical detection of biomarkers of oxidative stress

3.1. Electrochemical determination of oxidative protein damage Biomarkers

3.1.1. Protein carbonyls

As shown in Scheme 1 in the introduction, one of the outcomes of the oxidation of proteins via ROS and RNS is the formation of a reactive carbonyl group due to the oxidative deamination process [50]. This reaction occurs with an oxidation reaction in the presence of an H_2O molecule. Therefore, the oxidative stress status can be assessed by measuring the carbonyl-containing oxidized proteins.

Many chemical procedures were reported to measure protein carbonyls [51,52]. Design and construction of electrochemical biosensors to determine oxidized proteins with high sensitivity and low detection limits have also been reported. For example, an electrochemical sensor was designed based on the interaction between the oxidized Bovine serum albumin (BSAc) and 2,4-dinitrophenylhydrazine (DNPH, as a redox compound) [40]. First, the electrochemical behavior of DNPH was evaluated by cyclic voltammetry and differential pulse voltammetry (DPV) on a glassy carbon electrode in 50 µM DNPH at pH = 7.0, giving rise to an anodic peak observed at E_{pa} = +0.23 V vs Ag/AgCl. Then, a mixture of the 4-styrenesulfonic acid-Nafion matrix (SS-Nafion) was used to immobilize DNPH and modify the electrode surface.

The reactive carbonyl compound (BSAc) formed via the protein oxidation process is reacted with the hydrazine moiety of DNPH and created an imine compound (C=NH) (Fig. 7 I). As a result, the anodic current for DNPH at E_{pa} = +0.23 V was decreased. The native BSA shows no change in the electrical signal of the oxidation peak of DNPH (Fig. 7 IIA). By increasing incubation time, the anodic peak's current drastically decreased and disappeared (Fig. 7 II B). By analyzing BSAc at different concentrations, the sensitivity and detection limits were observed to be 0.015 nmol and 0.75 pmol, respectively (Fig. 7 II C, D).

Impedimetric sensing of several carbonyl compounds such as acetaldehyde, propanal, furfural, hexanal, heptanal, octanal, and nonanal has been performed based on the oxidation of hydrazone derivatives of aldehydes on glassy carbon electrodes by Boumya et al. [53]. The achievable linear range-extended between 30-1000 µmol L^{-1}, and limits of detection varied from 15.82 to 78.39 µmol L^{-1} for all aldehyde-2,4-DNPH. The sensor was successfully applied to determine aldehydes in orange juice but no information was given on its long-term operational stability. Saczk and coworkers combined electrochemical detection with a conventional separation method (HPLC) to quantify aldehydes such as butyraldehyde, 5-hydroxymethylfurfural, and 2-furfuraldehyde in foodstuffs [54].

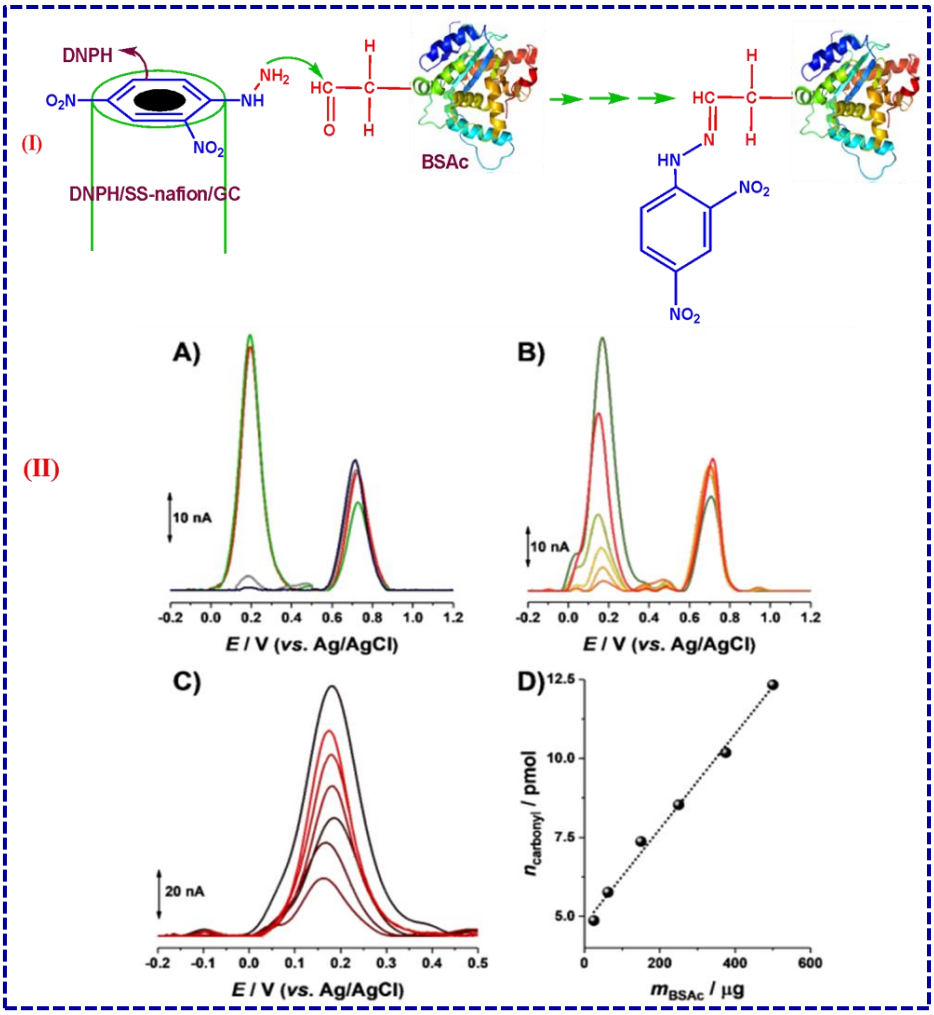

Fig. 7 (I) Electrochemical system for detection of oxidized protein (BSAc) on modified electrode. (II) DP voltammograms at DNPH/SS-nafion/GC in pH = 7.0 after incubation in: **A)** 1 mg mL^{-1} BSAc during (—) 0, (—) 30 and (—) 60 s, and in (—) 2 mg mL-1 BSA during 60s; **B)** 0.1 mg mL-1 BSAc during: 0, 20, 30, 60, 120 and 300 s (the peak current decreases in this order); **C)** different concentrations of BSAc between 50 and 1000 µg mL-1 during 20 s; and **D)**the corresponding calibration curve [40].

3.1.2. 3-Nitrotyrosine

Peroxynitrite (PN) is one of the most critical factors for the nitration of proteins either free or protein-bound. PN, a powerful oxidizing agent, can be produced in vivo by the reaction of nitric oxide radical (produced from L-Arginine) and superoxide anion radical (produced from the reduction of O_2) [55]. 3-Nitrotyrosine (3-NT) can change the structure and function of the protein and associated with a series of pathologies such as Parkinson's disease, Alzheimer's disease, cardiovascular, cancer, neurodegenerative diseases and atherosclerosis, acute and chronic liver diseases, diabetes, and aging [56]. Therefore, 3-NT protein is considered an

essential biomarker for oxidative stress and its measurement is essential to monitor human health [57]. Electrochemical determination of 3-NT protein [58] has many advantages such as high sensitivity, rapid, inexpensive, high selectivity, low detection limit, and no need for toxic solvent or catalyst compared to other methods [59] such as high-performance liquid chromatography [60], and gas chromatography-mass spectroscopy [61].

Martins et al. reported a paper-based electrochemical sensor to detect 3-NT [62] due to the attractive features of the paper material (high surface area, porosity, low-cost, light-weight, recyclability, and flexibility). In this work, the electrochemical oxidation of 3-NT was carried out by cyclic voltammetry and square wave voltammetry techniques. After optimizing conditions such as pH, potential scan rate, and supporting electrolyte, calibration curves were recorded in various 3-NT concentrations, which shows a linear range of response between 500 nM and 1 mM, and a detection limit as low as 49.2 nM. On the other hand, an electrochemical sensor based on the reduction of 3-NT was also developed [63]. To increase sensitivity, a pencil graphite electrode (PGE) was modified with imprinted bimetallic Fe/Pd (BI-Fe/Pd) nanoparticle and the sensing platform was prepared in four steps: i) polishing and ultrasonication of PGE in distilled water; ii) modifying the surface with BI-Fe/Pd nanoparticle by drop coating process; iii) polymerization with a mixture (acrylamide, 3-NT and modified Fe/Pd NP) and N-N'-methylene bisacrylamide (MBAA) as crosslinker; iv) preparation of molecular imprinted polymer (MIP) with the extraction of 3-NT and production of cavities (Fig. 8). This approach is more sensitive than non-imprinted polymers while measuring the 3-NT in biological samples. The calibration curve (Ip vs C) was obtained by square wave stripping voltammetry (SWSV) and differential pulse stripping voltammetry (DPSV) techniques, and low detection limits were achieved for both SWSV (1.20 µg L^{-1}) and DPSV (3.25 µg L^{-1}) (Fig. 9 A and B). Furthermore, the diffusion coefficient of 3-NT was determined to be 2.87×10^{-10} cm^2 s^{-1} by the chronocoulometry technique. The sensor response was kept after 45 days storage.

Similarly, an electrochemical sensor for 3-NT has been reported based on a combination of molecular imprinted polymer (MIP) with nanomaterials such as gold nanoparticles (AuNPs), multiwall carbon nanotube (MWCNT), and graphene oxide nanoribbons (GONRs) [64]. The electrochemical method coupled to HPLC was also reported to achieve the highly sensitive detection of 3-NT [65].

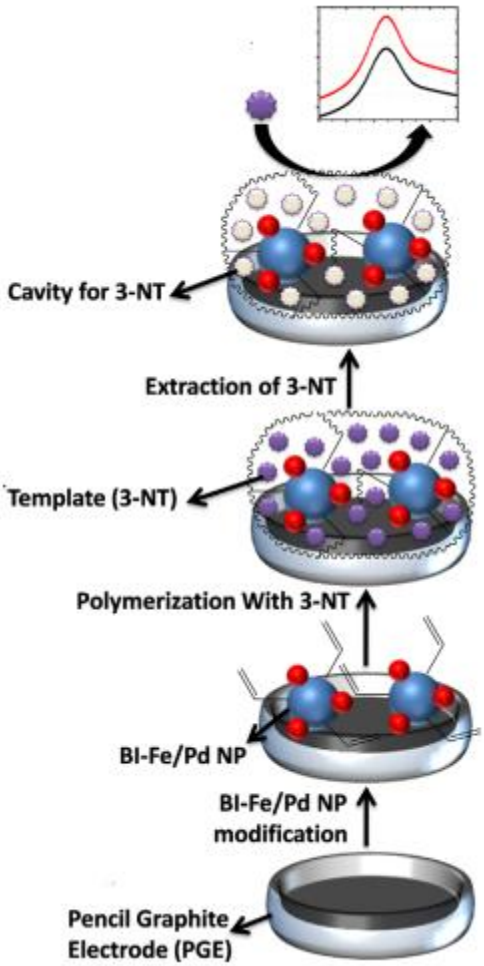

Fig. 8 The fabrication process of imprinted bimetallic Fe/Pd (BI-Fe/Pd) nanoparticle as a platform for the detection of 3-NT [63].

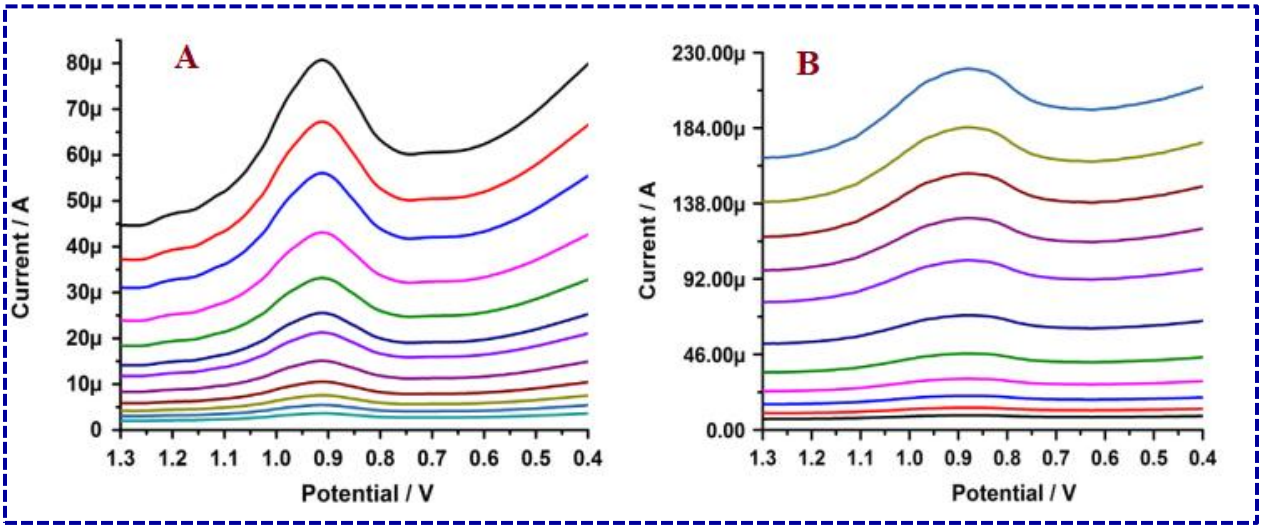

Fig. 9 (A) DPSV response of 3-NT on MIP-modified PGE with increasing concentration (9.90 µg L^{-1} to 867.57 µg L^{-1}), and (B) SWSV response of 3-NT on MIP-modified PGE with increasing concentration (4.90 µg L^{-1} to 867.57 µg L^{-1}) in optimized conditions [63].

3.1.3. Oxidized low-density lipoprotein (oxLDL)

The biological function of Low-density lipoprotein (LDL) is the transfer of cholesterol in plasma arteries which also contain proteins (e.g., apolipoprotein B-100) and lipids. In the presence of oxidizing agents (ROS or RNS), the native form of LDL changes to oxidized form (oxLDL), and the increase of LDL and oxLDL levels in plasma has a direct relationship with cardiovascular disease (atherosclerosis) [66]. Thus, the oxLDL or LDL level determination is a vital marker for the diagnosis of oxidative stress and cardiovascular events [67]. There are a vast number of diagnostic tools such as instrumental methods (enzyme-linked immunosorbent assay, supercapacitor-Based, proteomic, HPLC, and optical) and biomolecular electronic devices with different recognition parameters for prediction and determination of oxLDL and LDL concentration, as mostly analyzed by electrochemical impedance spectroscopy [68-73] (Table 2).

Table 2 Comparison of various electrochemical approaches for LDL detection.

Modified electrode	LOD (µM)	Linear range (µM)	Method	Reference
AAB/CNT-CH/ITO	12.5 mg/dL	0–120 mg/dL	EIS	[68]
AAB/PANI–SA LB	0.39	0.018-0.39	EIS	[69]
AuNPs-AgCl@PANI/GCE	0.34 pg/mL	0.34-13.4 pg/mL	EIS	[70]
AAB/NiO/ITO	0.015	0.018-0.5	EIS	[71]
PVF–AuNPs–MAb–BSA	3.50 µg/mL	3.50 -175 µg/mL	EIS	[72]
CYS/Au/mAb/SPE	0.22 µg mL^{-1}	0.50-18.0 µg mL^{-1}	EIS	[73]

AAB: anti-apolipoprotein B, CNT: carbon nanotubes, CH: chitosan, ITO: indium tin oxide, PANI: polyaniline, SALB: stearic acid Langmuir–Blodgett, AuNPs: Au nanoparticles, AgCl: silver chloride, GCE: glassy carbon electrode, NiO: nickel oxide, PVF: (polyvinyl formal), MAb: Monoclonal antibodies, BSA: Bovine serum albumin, EIS: electrochemical impedance spectroscopy.

In 2016, Kaur and coworkers developed an electrochemical immunosensing platform using the following steps, i) the deposition of semiconducting NiO thin film on ITO electrode via RF sputtering process; ii) the hydrolysis of NiO film to introduce OH functional group on the surface in H_2O_2/NH_4OH/H_2O (1:1:5 v/v) solution; iii) salinization of the hydrolyzed film by (3-aminopropyl)triethoxysilane (APTES) in toluene medium; iv) construction of immuno-electrode by immobilizing the antibody (AAB) in PBS consisting of 0.1 M NHS and 0.4 M EDC; v) incubation of LDL for electrochemical measurements (Fig. 10). The effectiveness of each preparation step has been demonstrated using FT-IR, SEM, AFM, and XRD analysis [74]. The measurement of current and resistance during the modification of the ITO electrode has been

carried out using cyclic voltammetry and electrochemical impedance spectroscopy (EIS), respectively. As shown in Fig. 11A, the voltammetric signal of the NiO/ITO electrode decreased upon immobilization of AAB due to blocked/hindered charge transfer. Consistent with this observation, the value of charge transfer resistance (R_{CT}) increased by coating AAB on the NiO/ITO electrode (Fig. 11B). The Nyquist plot was drawn for obtaining sensitivity, linear range, and detection limit in different concentrations of LDL on the AAB/NiO/ITO electrode at room temperature (Fig. 11C, D), and obtained 12 kΩ μM^{-1}, 0.018–0.5 μM, and 0.015 μM, respectively, with a long shelf life (18 weeks).

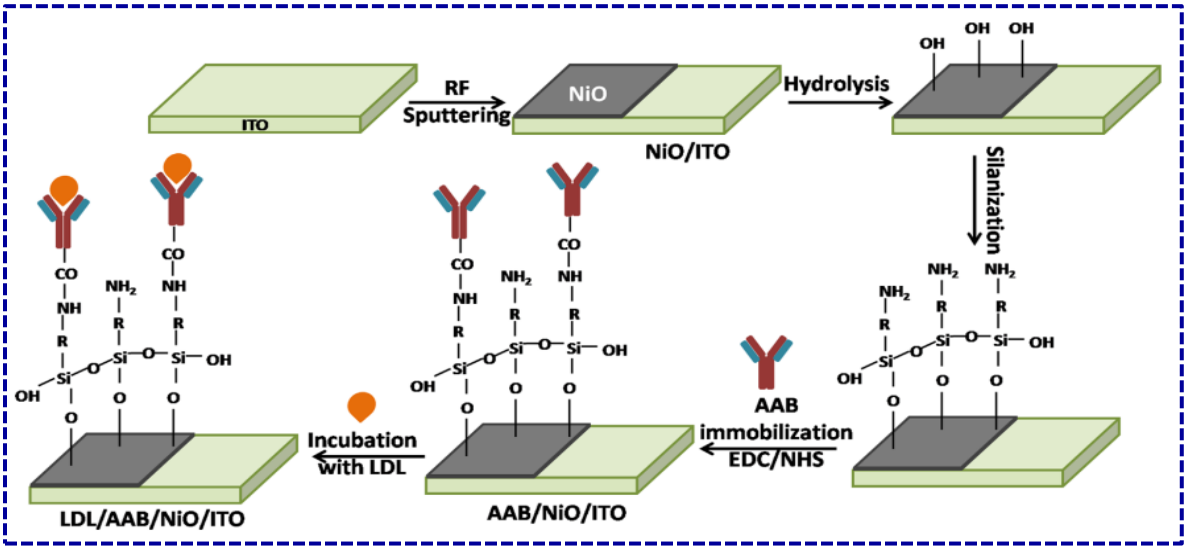

Fig. 10 Schematic for the preparation of the immune-electrode and binding of LDL with the antibody AAB [74].

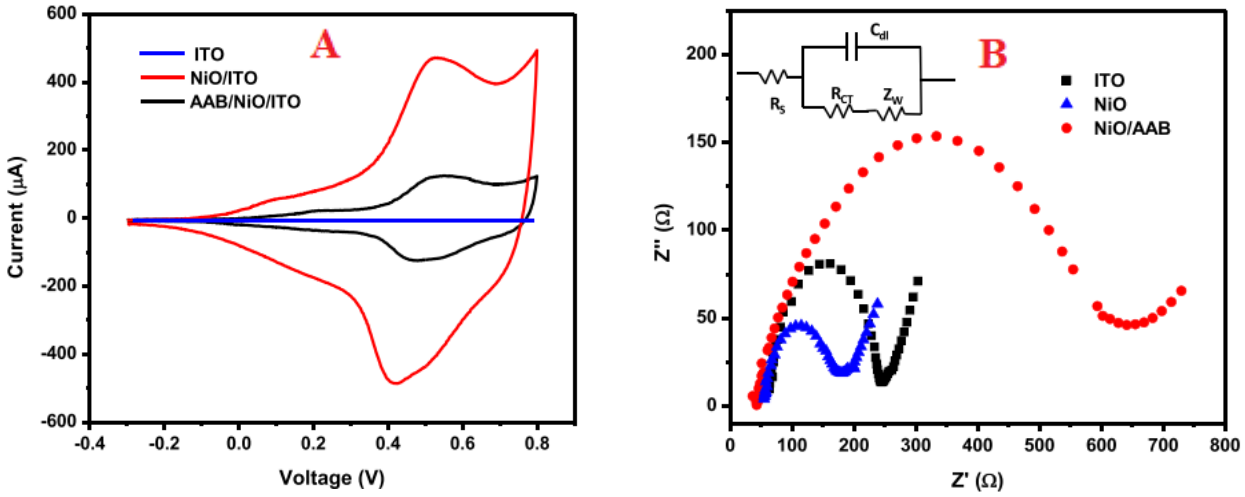

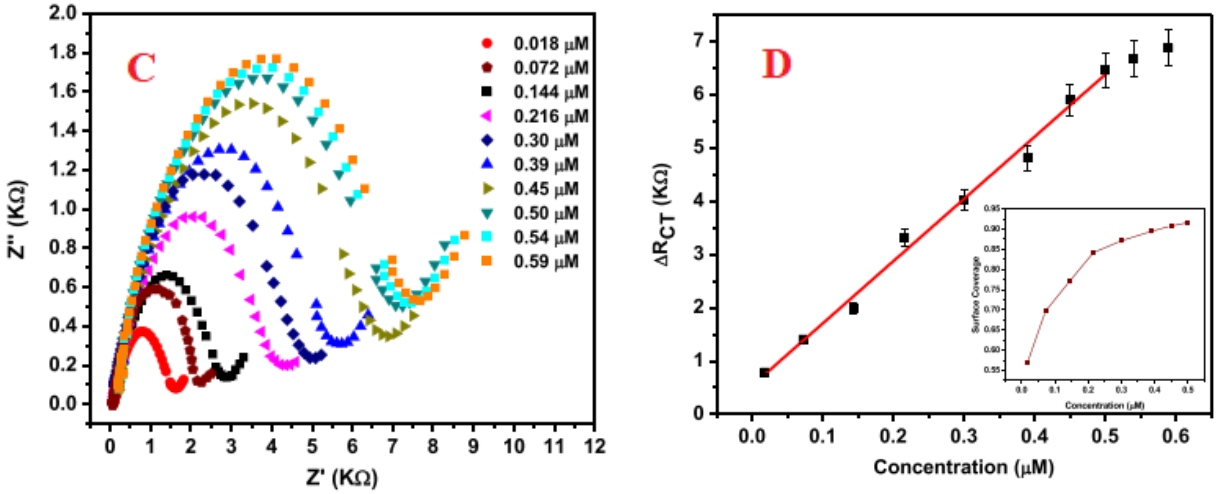

Fig. 11 (A) Cyclic voltammograms and (B) EIS of bare ITO/glass, NiO/ITO electrode and AAB/NiO/ITO immune-electrode. Inset B: shows the equivalent Randles circuit. (C) Impedimetric response studies of AAB/NiO/ITO immune-electrode incubated with different concentrations of LDL (D) Calibration curve obtained between ΔR_{CT} and concentration of LDL. Inset D: shows the variation of surface coverage of prepared immune-electrode versus concentration of LDL [74].

3.2. Electrochemical determination of oxidative lipid damage Biomarkers

In this section, we describe the electrochemical detection of lipid biomarkers such as malondialdehyde, methylglyoxal, 4-hydroxy 2-nonenal, and 2-Propenal.

3.2.1. Malondialdehyde

One of the most important lipid peroxidation biomarkers of oxidative stress is malondialdehyde (MDA) This compound is one of the final products of oxidation of Arachidonic acid (AA) (unsaturated fatty acid) [75]. MDA is an α-β unsaturated aldehyde, which causes both initiation and progress of many human troubles such as Alzheimer's disease, cancer (such as gastric and skin), liver disease, paranoid schizophrenia, Parkinson, diabetes, asthma, nephropathy, hypothyroidism, and cardiovascular disease [76]. Hence, the oxidative stress status can be identified via the determination of MDA level in the biological system, and therefore, the development of methods to measure MDA in plasma, serum, and gingival fluid is essential. Chemical and electrochemical procedures have been developed to detect lipid oxidation adducts. Chemiluminescence [77], Raman spectroscopy [78], HPLC with fluorescence detection, gas chromatography with mass detection [79], and spectrophotometry have been used so far, however, these techniques are limited due to poor sensitivity, less specificity, longer analyze time, and required more expensive instruments. The electrochemical methods overcome all these

setbacks. Yuan and coworkers designed a novel label-free electrochemical biosensor for detecting MDA using MWNTs [80]. Briefly, the GCE was modified with MWNTs in the presence of chitosan (CS). Then covalent adsorption of glutaraldehyde (GluA) and complement factor H (CFH) via formation of imine moiety, followed by dropping the MDA and BSA at the modified electrode (Fig. 12). The CS, GluA, and BSA, act as biocompatible, linkage, and blocking agents, respectively during the biosensor construction. The utilization of nanomaterials reduces resistance (EIS assay) or increases electrical conductivity (CV assay) of the biosensing electrode.

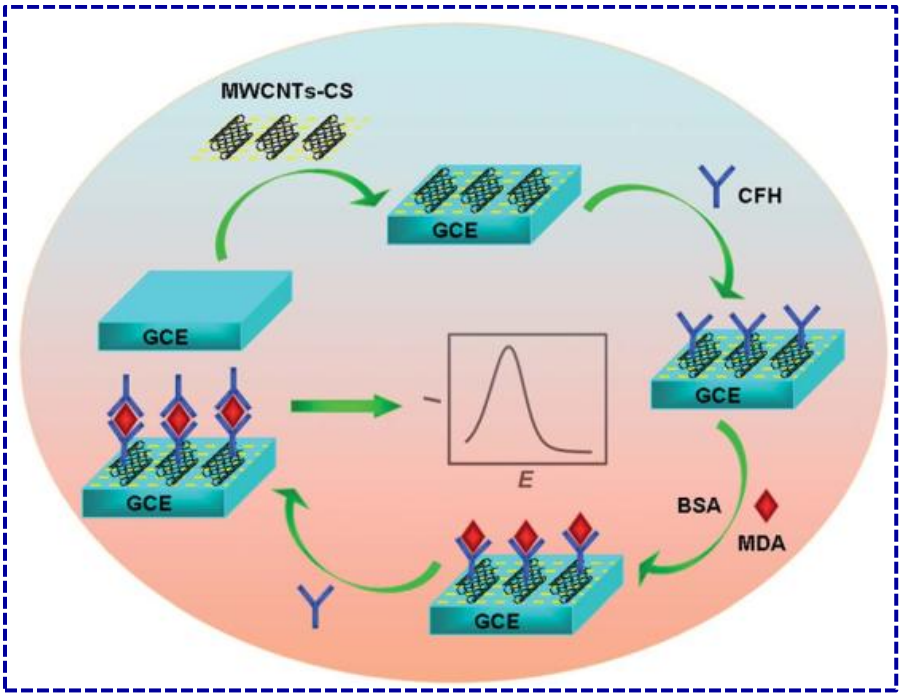

Fig. 12. A schematic diagram of the construction of the label-free biosensor for the detection of MDA [80].

The electrochemical assessment (the measurement of current and resistance) of each preparation step was performed by EIS and CV analysis (Fig. 13). The presence of MWNTs accelerates the electron transfer reaction rates (with a concomitant decrease of the semicircle diameter of Nyquist plots) whereas further modification (coating of GLD, CFH, and BSA) resulted in lower voltammetric currents and larger charge transfer resistance because of the existence of blocking agents onto the sensing platform. Using differential pulse voltammetry the detection limit and linear concentration range were estimated to be 0.047 μmol^{-1} and 0.1-90 μmol^{-1}, respectively, but no information was given on the stability [80].

The preparation of nanocomposite by combining polymers and nanomaterials using layer by layer strategy offers remarkable conductivity and electroanalytical properties for biosensors. In recent years, quantum dots and poly amino acids (polyarginine) have been utilized to identify

MDA in exhaled breath condensate samples using differential pulse voltammetry [81] and achieved a detection limit as low as 0.329 nM. In another approach, Hasanzadeh and his team reported the electrochemical behavior of MDA on polytaurine modified gold (PT/Au) and found that the PT/Au electrode is appropriate for detecting MDA in exhaled breath condensate and serum samples with a linear response in the 0.78-3.10 mM concentration range and a detection limit of 34 nM, with acceptable stability (90% after 100 analyses) [81]. In these examples, the benefits of conductive polymers and quantum dots (such as adjustable electrical conductivities, high surface area, and surface/volume ratio, numerous active sites) are responsible for the enhanced performance of the sensors.

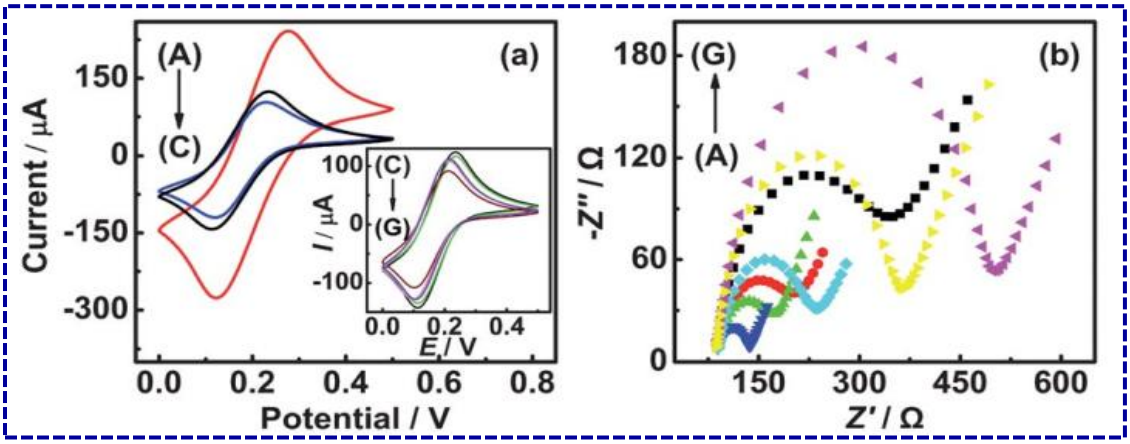

Fig. 13 CVs (a) and Nyquist diagrams (b) of GCE/MWNT–CS/(A), bare GCE (B), GCE/MWNT–CS/GLD (C), GCE/MWNT–CS/GLD/CFH (D), GCE/MWNT–CS/GLD/CFH/BSA (E), GCE/MWNT–CS/GLD/CFH/BSA/MDA (F) and GCE/MWNT–CS/GLD/CFH/BSA/MDA/CFH (G) in 5 mmol L^{-1} $K_3Fe(CN)_6/K_4Fe(CN)_6$ (1:1) containing 0.1 mol L^{-1} KCl [80].

3.2.2. Methylglyoxal

Methylglyoxal (MG) is a biomarker of diabetes (type 2) and aging (Alzheimer's disease) in medical diagnostics. MG is mainly generated by fatty acids, amino acids, and glucose metabolisms, according to pathways involving enzymatic and non-enzymatic reactions. One of the primary sources of MG production is lipid peroxidation by the oxidative stress process [82]. At an excessive level within the blood plasma (more than 0.7 μM), MG introduces non-compensatory damages to the biological system such as variation of the physicochemical properties of proteins and DNA [83]. On an indirect route, after the production of MG by the lipid peroxidation, a non-enzymatic reaction between the carbonyl moiety of MG and the amine group of proteins can occur, which consequently produce advanced glycation end-products (AGEPs). AGEPs induce oxidative stress by increasing levels of ROS and RNS, thus initiating some diseases such as diabetes, Alzheimer's disease, and aging (carbonyl stress).

Due to the exponential increase in the concentration of ROS and RNS in the MG production cycle, rapid and in-situ monitoring of MG is vital. In addition to expensive and time-consuming chemical methods such as gas chromatography, capillary electrophoresis, colorimetry, or high-performance liquid chromatography (HPLC) [84], electrochemical sensors and biosensors based on enzymatic and non-enzymatic electrodes have been used for the determination and detection of MG. Wu et al. detected MG by square wave voltammetry using a GCE modified with chitosan nanosphere-carboxymethyl cellulose-carboxyl-functionalized multi-walled carbon nanotubes (CSN-CMC-MWCNTs-COOH) [85,86]. The sensor was used to measure the MG in a honey sample within the range of a 5×10^{-8} – 8×10^{-4} mol/L, and a detecting limit of 9.6×10^{-9} mol/L with good stability (98.5 % after 15 days storage at 4°C [86]). Chatterjee and coworkers developed a single-walled carbon nanotube modified glassy carbon electrode (SWCNT-GCE) to detect MG by cyclic and square wave voltammetry. This sensor exhibited a rapid response, good stability, selectivity and reproducibility, high sensitivity (76.3 nA mM^{-1}), and a wide linear range (0.1 to 100 mM). Then, the MG level in human plasma was also measured. Besides SWCNTs, metal oxide nanoparticles such as ZnO [87], V_2O_5, and CeO_2 can also be exploited in electrochemical sensors to enhance the electrocatalytic and sensitivity for the detection of MG. Alagappan et al. designed an electrochemical non-enzymatic sensor using Pt electrode modified with GSH cofactor and V_2O_5 nanoparticles for MG detection in rice samples [88].

Furthermore, Ramachandra Bhat and coworkers reported an electrochemical enzymatic sensor based on CeO_2 (as nano-interface), GSH (as a cofactor), and glyoxalase1 (GLO 1) (as an enzyme), for the sensitive determination of MG in Cow Milk (LOD: 2.14 nM; linear range: 5-50 µM) [89]. The proposed detection mechanism is as follows: 1) the GSH is oxidized to GSSG according to a reversible process involving the exchange of two electrons and two protons; 2) after adding MG to the solution, the oxidized glutathione (GSSG) reacted with MG to form hemithioacetal (HTA). In the presence of GLO 1 on the electrode surface, HTA is further transformed to give the final product, namely S-D-lactoylglutathione (Fig. 14).

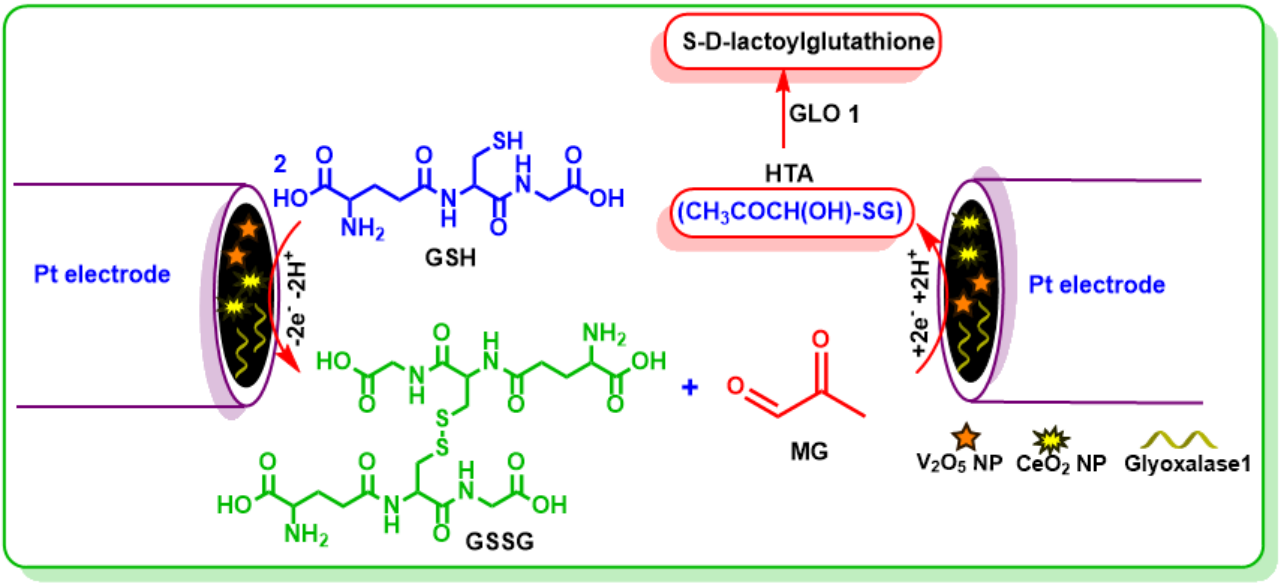

Fig. 14 Electrochemical detection of MG base on oxidation of GSH at modified electrodes with metal oxide nanoparticles and enzymes [88]**.**

3.2.3. 4-hydroxy 2-nonenal

4-hydroxy 2-nonenal (HNE) is a reactive product of lipid peroxidation, originating from non-enzymatic radical chain reactions such as arachidonic acid or linoleic acid with ROS [90]. HNE, a reactive α, β-unsaturated aldehyde, can undergo many different reactions such as reduction, oxidation, epoxidation, and Michael additions. 1,2 and 1,4 nucleophilic addition reaction in the presence of nucleophilic thiols (Guanine and Cysteine) or amines (Guanine, Adenine, Cytosine, Arginine, Lysine, and Histidine) occur in proteins, nucleic acids, and central nervous system (Amyloid-β peptide). Additionally, after 1,4 Michael addition reaction, the formation of a cyclic hemiacetal compound is possible through an intramolecular nucleophilic reaction of the hydroxyl group in C-4. These products are known as advanced lipoxidation end-products (ALEPs) [91].

Because of the harmful biological effects of HNE, the identification and measurement of this carbonyl reactive species are of crucial importance. Goldring and coworkers reported a high-performance liquid chromatography coupled with electrochemical (HPLC-EC) to detect HNE in the liver sample [92]. They used 2,4-dinitrophenyl hydrazine(DNPH) as a probe, and the sensitivity of this method is more significant than UV and GC/MS methods. HPLC-EC method shows a low detection limit in the range of 0.5-1 pM. Because the C-1 of HNE is a redox center, electroanalysis might be exploited in the future for remote sensing in oxidative stress monitoring.

3.2.4. 2-Propenal (Acrolein)

Among the four vinyl aldehydes compounds obtained via lipid peroxidation, Acrolein possesses the highest toxicity in biological systems due to its high reactivity with thiol (-SH) and amine (-

NH_2) moieties in macromolecules (DNA, protein) [93]. Three relevant sources of Acrolein include exhaust gas in air, blood and serum samples, and foodstuff Due to the biological and environmental importance of Acrolein and its relation with the various diseases such as Alzheimer's, aging, atherosclerosis, and cancer, analytical procedures (luminescence, gas chromatographic, HPLC-UV, colorimetry, GC-MS, electron impact mass spectrometry, electron capture detection), alone or coupled with electrochemical methods, have been reported for the sensitive and selective detection of Acrolein in intended samples.

An extensive investigation of Acrolein and unsaturated aliphatic aldehydes detection by hyphenated methods was carried out by Casella and his coworkers [94]. They obtained a detection limit of 0.15 µM for Acrolein analysis in a heated vegetable oils sample by liquid chromatography coupled to a pulsed electrochemical method (amperometric sensor) at a polycrystalline platinum electrode. In another study, they used HPLC-pulsed amperometry to detect and measure aliphatic aldehydes such as formaldehyde, propionaldehyde, acrolein, valeraldehyde, and acetaldehyde using a platinum electrode (detection limit < 2.5 µM). Dossi et al. reported a procedure based on microchip electrophoresis with electrochemical detection for the determination of aliphatic aldehydes such as 2-propenal, formaldehyde, and acetaldehyde, in air samples. In this study, 2,4-dinitrophenylhydrazine (DNPH) was used as a probe, and hydrazine derivatives resulting from the reaction with aldehydes were used for electrophoresis and electrochemical measurements [95]. The detection limit and linear range were calculated as 9.2 µM and 2–100 mg/mL, respectively, in 15 mM borate buffer (pH= 9.2) using a GCE. Even if no real long-term stability data were provided, the detector seemed to be quite stable as it allowed of 11 repetitive chromatographic experiments (~3 h of operation time) with relative standard deviations of 1.3% for maleic acid and 6.8% for lactic acid.

3.2.5. 8-isoprostane and F2-isoprostanes

In addition to unsaturated aldehydes in the preceding section (malondialdehyde, methylglyoxal, 4-hydroxy 2-nonenal, and acrolein), isoprostanes are important biomarkers of lipid peroxidation with a higher molecular mass for assessment and diagnostic of oxidative stress [96]. 8-isoprostane [97] and F2-isoprostane are two types of lipid oxidation in vivo products that are likely to be used for the identification of the oxidative stress status within blood and saliva samples. This should be possible due to their unique properties such as their existence at measurable amounts in the biological system, their good chemical stability, and their use as specific biomarkers as their concentration levels are expected to rise with the oxidation of lipids. In addition, increasing ROS levels can produce isoprostanes, which are possibly involved in physical and mental diseases such as HIV, renal, diabetes, aging, pulmonary, neurological, prostate cancer, or cardiovascular increases [98]. Sanchez-Tirado et al. have revolutionized the chemical approaches to detect and determinate 8-isoprostane by using electrochemical immunosensors [99]. The procedure for the preparation of the competitive immunoassay is presented in Fig. 15. Briefly, carboxylate carbon nanohorns were immobilized on the screen-

printed electrode and activated using 1-ethyl-3-(3-dimethylaminopropyl) carbodiimide (EDC) and N-hydroxysulfosuccinimide (NHSS) compounds. Then, it was incubated in BSA as a blocking agent followed by adsorption of antigen (ISO) and HRP-labeled antigen (HRP-ISO) onto the modified electrode surface. Amperometric measurements (at an applied potential of -200 mV) were carried out in the presence of hydroquinone (HQ) and H_2O_2 as redox mediators and HPR substrate, respectively. The detection limit of 8-isoprostanes in two human serum samples was excellent (12 pg/ml), with long stirage stability (30 days). In another approach, Lee et al. developed a portable electrochemical sensor (three-electrode system) coupled with a microfluidic system to detect and measure pulmonary hypertension biomarkers such as 8-isoprostane, low-density lipoprotein (LDL), fibrinogen, and adiponectin in clinical diagnosis [100]. All these biomarkers were analyzed by cyclic voltammetry and square wave voltammetry, and the obtained detection limit is nearly 1 µg/mL, without however any stability data provided.

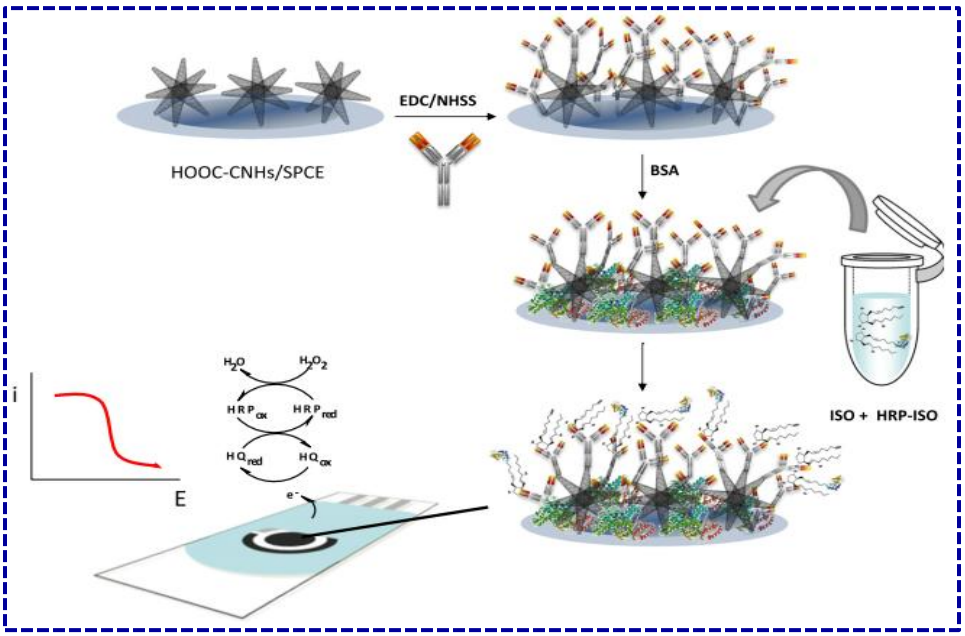

Fig. 15 Schematic display of the different steps involved in the preparation and functioning of the anti-ISO-CNHs/SPCE immunosensor for detection of 8-isoprostane [99].

3.2.6. Thiobarbituric acid-reactive substances

Thiobarbituric acid-reactive substances (TBARS) are by-products or standard biomarkers for the lipid peroxidation-induced reactive oxygen species [101]. TBARS are used for monitoring lipid oxidation status according to direct and indirect strategies. 2-thiobarbituric acid (2-TBA), an electroactive compound, can directly be determined with electrochemical techniques. Vaneesorn and Franklin Smyth carried out an electrochemical study of 2-thiobarbituric acid derivatives in the pH range of 4-l 2 using a hanging mercury electrode by cyclic voltammetry and cathodic stripping voltammetry [102]. They reported linear concentration ranges for these derivatives

between 0.242 to 4.84 ppm. Shahrokhian et al. reported the electrochemical behavior of 2-TBA on carbon paste electrode (CPE) using cyclic voltammetry [103], in which cobalt phthalocyanine (CoPc) was used as a modifier to increase electrocatalytic properties of CPE. Subsequently, the sensitivity was enhanced to measure 2-TBA in human serum samples. Consistent with the Pourbaix diagram ($E_{pa/2}$-pH), the anodic peak shifted to a less positive potential with increasing pH (participation of H^+ in the oxidation process) and, at pH>10, the oxidation of 2-TBA was no more pH-dependent. The detection limit of 0.07 mM was obtained using differential pulse voltammetry. You et al. decreased the LOD of 2-TBA down to 0.1 µM via hydrodynamic voltammetry (carbon fiber microdisk electrode) coupled with capillary electrophoresis technique [104]. Numerous chemical and electrochemical studies have been reported for indirect analysis of 2-TBA in different matrixes (Plasma, Saliva, Serum, Serum, Seminal), with good operational stability of the end-column electrochemical detector after proper activation of the carbon fiber electrode [104].

Similar to 2-TBA, $(TBA)_2$-MDA is also electroactive and such species can be used as a probe to detect non-electroactive aldehydes via electrochemical methods. In this way, Zhang et al. developed a combinatorial strategy (amperometric coupled with the capillary electrophoretic method) to identify non-electroactive aldehydes (butanal, propanal, formaldehyde, etc.) in the concentration range between 0.008 and 0.074 mg/L [105].

3.3. Electrochemical determination of oxidative DNA damage Biomarkers

3.3.1. Electrochemical determination of 8-hydroxy-deoxyguanosine (8-OHdG)

Responsible nitrogenous bases for the transmission of genetic information (purine and pyrimidine bases) changes to oxidized form when the concentration of ROS (free radicals and non-radicals) is high in the human body [106]. Guanine has the lowest oxidation potential between four nucleic acid bases; therefore, it oxidizes to 8-hydroxydeoxyguanosine (8-OHdG) in the presence of ROS. This phenomenon causes mispairing in the structure of the double helix and subsequently disrupts in transcription and protein production process. As a consequence, high levels of nucleotide oxidation or increasing 8-OHdG concentration in the body may lead to some diseases such as cancers, Parkinson's, diabetes, and atherosclerosis [107].

Numerous electrochemical approaches have been reported for the detection of 8-OHdG as a vital biomarker of DNA damage [108,109]. The essential factor in these studies is the improvement of sensitivity and selectivity for 8-OHdG, which can be achieved via modifying recognition elements (working electrodes) with carbon and metal nanoparticles, polymers, and biological compounds (aptamer and DNA). The various approaches for detecting 8-OHdG and diagnosis of oxidative stress are summarized in Table 3 [110-121]. The three mainly used electrodes are GCE, Au, and SPE, and are usually modified with carbon or nano carbon-based materials (CNTMW, and Gr), biological elements (aptamers), metal oxides (TiO_2, and ZnO), or

conductive polymers such as (poly(3-methylthiophene) and poly(indole-5-carboxylic acid)), as recognition elements. They enable the detection of 8-OHdG in the nM concentration range (see some data in Table 3 and a more comprehensive list in Table S3 in SI).

For example, Zhang et al. developed a spectroelectrochemical immunosensor based on a "core-shell" structure to detect 8-OHdG with high selectivity and sensitivity (0.085 ng mL^{-1}) (Fig. 16) [119]. The gold/silica/quantum dots (Au/SiO_2/CQDs) core-shell nanoparticles were prepared first in the presence of (3-aminopropyl)trimethoxysilane (APS) and then coated onto the Pt electrode surface. After drying at room temperature, the electrode surface was activated using EDC and NHS followed by immobilization of Rabbit anti-8-OHdG (Ab) and Bovine serum albumin (BSA) (as a blocking agent) on the surface (Fig. 16 step B). This electrode was used as an anode in electrochemiluminescence immunosensor (ECL) in phosphate buffer solution (PBS, 0.1 mol L^{-1}, pH=7.4) containing 0.05 mol L^{-1} potassium persulfate ($K_2S_2O_8$). In the presence of 8-OHdG, the active surface of the modified electrode was progressively blocked and the ECL signal intensity decreased proportionally to the analyte concentration (Fig. 16 step C). The operational stability was acceptable (8.5 % RDS for 16 cycles of continuous potential scans) and the life time of the immunosensor was 30 days when stored at 4°C.

Table 3 A comparison of electrochemical sensing devices reported for the detection of 8-OHdG in terms of linear concentration range, measurement method, and limit of detection.

Modified electrode	**LOD (µM)**	**Linear range (µM)**	**Method**	**Reference**
GCE/CNT-PEI	0.1	0.5-30	DPV	[110]
ZnO NFs@GOS/SPCE	0.008.67	0.05-536.5	CV-AM	[111]
SWCNTs-Nafion/GCE	0.008.0	0.03-1.25	DPV	[112]
GCE/P-Arg/ErGO-AuNPs	0.001	0.001–0.1	DPV	[113]
ss-DNA/GNs/GCE	0.00875	0.0056–1.155	CV	[114]
Gr/PEDOT/CNTMW/COOH	0.74 ng/ml	5.0-1000 ng/ml	DPV	[115]
PICA/CHI/GCE/PA	30.0 pg/ml	0.1-10000 ng/ml	IS-DPV	[116]
PSWNT/GCE	0.001	0.003-3.061	LSV	[117]
MWNT-DHP/GCE	0.009	0.0008-5.0	LSV	[118]
Au/SiO_2/CQDs	0.085 ng/ml	0.2-200 ng/ml	ECL	[119]

Ag–TiO_2–rGO/SPE	0.01	0.05–25	DPV	[120]
SPE-Gr	0.09	0.3-100	LSV	[121]

GCE: glassy carbon electrode; CNT-PEI: carbon nanotube- polyethylenimine; DPV: differential pulse voltammetry; ZnO NFs@GOS/SPCE: zinc oxide nanoflower @graphene oxide sheet/screen printed electrodes; CV-AM: cyclic voltammetry-amperometry; SWCNTs: single wall carbon nanotubes; P-Arg: poly (L-arginine); ERGO: electrochemically reduced graphite oxide; AuNPs: gold nanoparticles; ss-DNA/GNs: single-stranded DNA/ graphene nanosheets; PEDOT/CNTMW: poly(3,4-ethylenedioxythiophene)/carbon nanotubes multi-walled; PICA/CHI: Poly(indole-5-carboxylic acid) (PICA)/chitosan; IS: immunosensor; PSWNT: porous single-walled carbon nanotubes; LSV: linear sweep voltammetry; DHP: dihexadecyl hydrogen phosphate; CQDs: carbon quantum dots; ECL: electrochemiluminescence; rGO: reduced graphene oxide; SPE: screen-printed electrode, Gr: graphene.

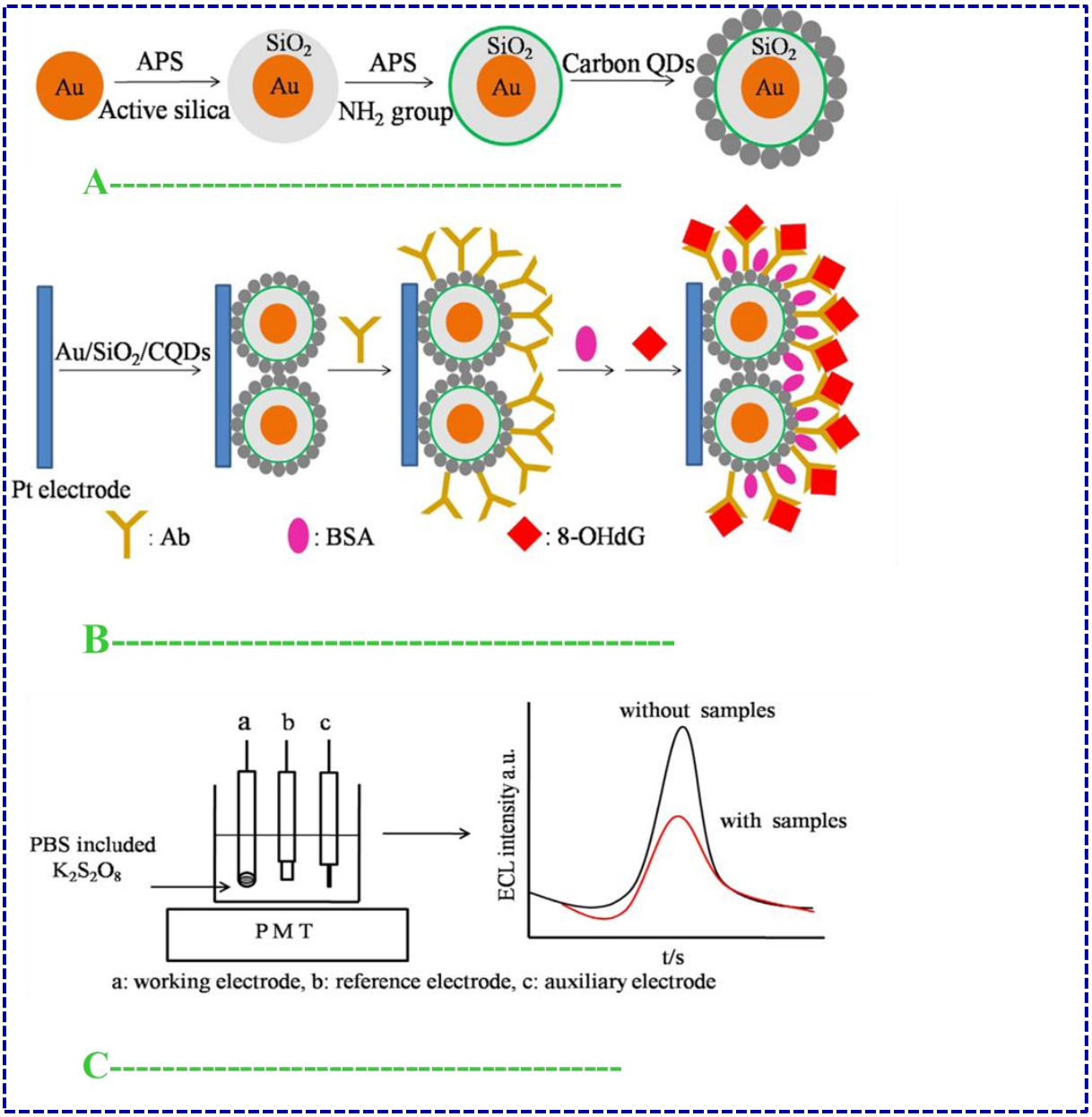

Fig. 16 The Schematic of preparation procedures of A) $Au/SiO_2/CQDs$ core-shell nanoparticles B) ECL electrode modified by $Au/SiO_2/CQDs$ core-shell nanoparticles and antibody and C) spectroelectrochemical system and detection procedure. The voltage of the photomultiplier tube (PMT) was 600 V [119].

4. Electrochemical determination of endogenous (enzymatic) antioxidants

4.1. Glutathione (reduced GSH/ oxidized GSSG)

Glutathione (GSH), a powerful antioxidant agent, acts as anti-oxidative stress in every cell and pharmaceutical sample [122]. GSH is converted into an oxidized form (GSSG) and combated

with active free radicals (ROS or RNS) in the body. The measurement of GSH or the ratio of reduced to oxidized form is appropriate to diagnose the antioxidant level and oxidative stress status [123]. The overall oxidation reaction of GSH with H_2O_2 or other active particles is illustrated below.

There are several chemical methods such as fluorescence, fluorometric, HPLC, capillary electrophoresis, UV-Visible Spectroscopy (UV-Vis), flow cytometric, electron paramagnetic resonance, and liquid chromatography coupled to isotope ratio mass spectrometry reported for in-vivo and in-vitro GSH measurements or the ratio of oxidized/reduced GSH [124]. On the other hand, GSH can be measured by its oxidation or reduction current corresponding to the concentration in the matrix. Several electrochemical sensing techniques have been reported so far for the electrochemical determination of GSH and its antioxidant activity. For instance, in 2012, Harfield and coworkers reported the determination of GSH or glutathione disulfide using amperometry and voltammetry [125]. In this work, different electrochemical protocols and strategies reported after 2012 were highlighted. It is well known that the enzymes, polymers, and redox mediators on different electrode matrices improve the sensitivity. Lee et al. presented a modified GCE via carbon nanotubes and polycaffeic acid to detect GSH [126], and achieved a detection limit as low as 500 nM. A variety of redox mediators such as catechol derivatives, 4-aminophenol, and chlorogenic acid have been used for the determination and separation of GSH in human samples. Also, the GSH/GSSG ratio is a critical parameter to estimate the activation or inactivation of oxidative stress in cells. Childs et al. have measured this ratio in prostate cancer cells via HPLC coupled with the electrochemical method [127]. Total sulfide and disulfide concentrations are determined using colorimetry. The detection limit and linear range of GSH and GSSG are 1.2, 1.1 nM, and 2.3-1197.4, 2.4-1248.3nM, respectively. The analytical parameters of some other electrochemical sensing or biosensing devices for GSH [128-140] are listed in Table 4 (see more comprehensive list in Table S4 in SI).

The optimum condition (no oxidative stress) for GSH/GSSG ratio is 100:1 in cells and this ratio decreases during oxidative stress. Lei et al. was observed the decrease of this ratio in cancer cells [128]. The electrode was prepared by various steps as shown in Fig. 17. At first, the hammers procedure was used to synthesis graphene oxide (GO) from graphite powder, followed by the chemical reduction and nitrogen boron doping processes leading to the formation of N, B-rGO nanocomposites. To obtain a larger area, iron phthalocyanine (FePc) was coated on N, B-rGO with π–π interaction. Electrochemical oxidation of GSH has been carried out on a modified electrode in 0.01 M phosphate buffer saline and observed the anodic current corresponding to the concentration of GSH. The lower detection limit of 7.1×10^{-9} M and the linear response of 5.0×10^{-8} M to 1.6×10^{-3} M were achieved, with an excellent anti–interference performance and good long–term stability (95% after 20 cycles).

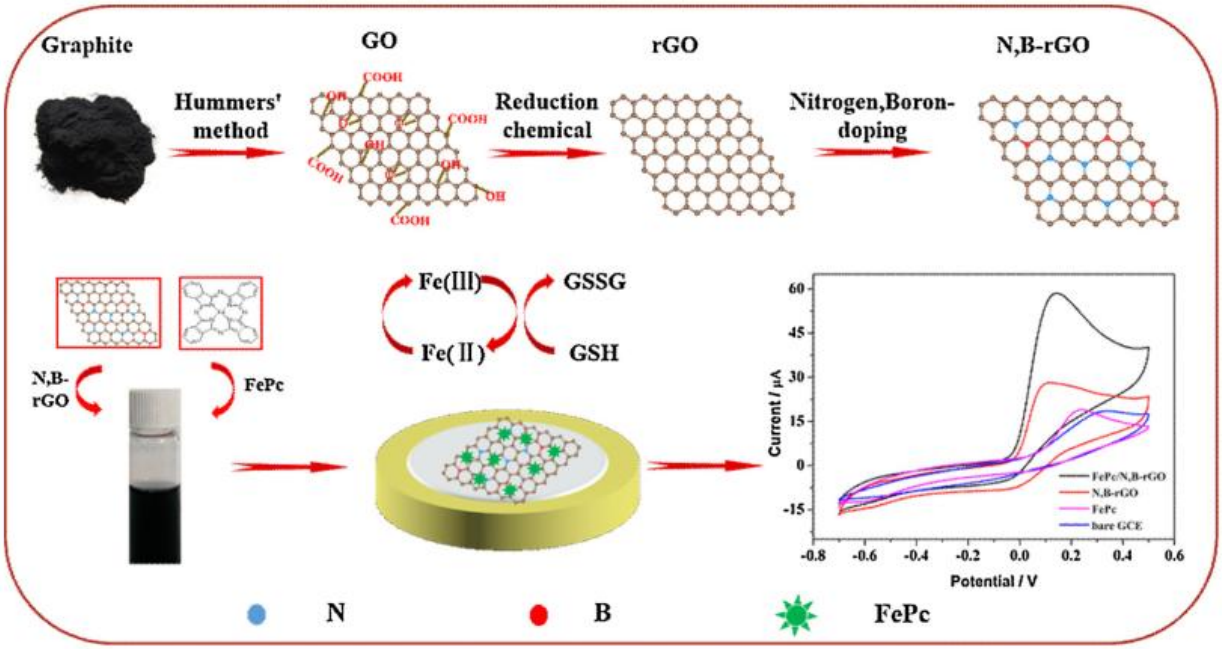

Fig. 17 Preparation and application of the FePc/N, B–rGO nanocomposite [128].

Table 4 A comparison of electrochemical sensing devices reported for the detection of glutathione, comparing factors such as the electrode, linear range, measurement method, and limit of detection.

Modified electrode	LOD (μM)	Linear range (μM)	Method	reference
MWCNT@rGONR/GCE	0.039	0.05-266.3 mM; 266.3-766.3 μM	AM	[129]
MnO_2 nanosheets	0.0037	0.010-2	ECL	[130]
NiHCF/CTAB/AuNPs	0.08	0.2–1	DPV	[131]
TChPRu-MWCNT/PE	0.3	0.6–56.8	DPV	[132]
$AgNPs_{(TMSPED)}$-rGO/ GC	0.1	0.1-2.75	AM	[133]
MWNTs/CoQ10/IL	0.00032	0.0040-0.2	DPV	[134]
MWCNT/ CPE	264.2	25-800	DPV	[135]
SPCE-G	2	2-12	CV	[136]
Sb_2O_3–CPE	0.34	2-200	SWV	[137]
AgNCs/AgNPs/GO	0.0343	0.1–1	PEC	[138]
c-MWCNTs/DPBDF/GCE	0.73	1.0-100.0	DPV	[139]

MoS_2 nanosheet	0.703	10- 500000	AM	[140]

MWCNT: multiwalled carbon nanotubes, rGONR: reduced graphene oxide nanoribbons core-shell heterostructure, AM: amperometry, ECL: electrochemiluminescence, NiHCF: nickel hexacyanoferrate, CTAB: cetyltrimethylammonium bromide, AuNPs: Au nanoparticles, DPV: differential pulse voltammetry, TChPRu: trichloro(terpyridine)ruthenium(III), PE: paste electrode, $AgNPs_{(TMSPED)}$-rGO: silver nanoparticles anchored reduced graphene oxide, CoQ10/IL: coenzyme Q10/ionic liquid, SPCE: screen printed carbon electrode, CV: cyclic voltammetry, CPE: carbon paste electrode, SWV: square wave voltammetry, PEC: Photoelectrochemistry, DPBDF: (2Z,4E)-3-(3,4-dihydroxyphenyl)-1,5-bis (2,4-dinitrophenyl)formazon.

4.2. Cysteine

Cysteine (CyS), a thiol-containing amino acid, is an endogenous antioxidant and valuable biomarker to monitor oxidative stress status in saliva, serum, urine, and plasma [141]. The abnormal level of CyS is associated with oxidative stress-induced different diseases or disorders and can serve as a signal to diagnose oxidative stress in biological samples [142]. Although various chemical techniques have been reported for quantification of CyS, electrochemical procedures are preferable because of noteworthy features such as low cost, simplicity, excellent sensitivity, ease of construction, and selectivity. A wide spectrum of composite films or electrochemical platforms has been designed with mediators, polymers, and nanomaterials to decrease the overpotential for the oxidation process of CyS [143]. Some methods or systems such as capillary zone electrophoresis and flow injection have been combined with the electrochemical assay for the identification of CyS in desired samples [144]. Mani et al. have developed a GCE that consists of graphene oxide (GO) nanoparticles and tetraamino-functionalized cobalt phthalocyanine (pTACoPc) to monitor CyS and hydrazine concentration in biological and water samples [145]. pTACoPc was coated using electrodeposition technique in the potential range 1.0 to -2.6 V vs Ag|AgCl (saturated KCl) in DMSO solution (Fig. 18). The optimum of 20 cycles was found to obtain the maximum anodic peak current (Fig. 18 inset). A good storage ability was reported (94.28% after one month), as well as a acceptable operational stability (6.4% signal loss after 200 cycles).

The electrochemical behavior of CyS was studied using the modified electrodes at pH=7 (Fig. 19). The electrocatalytic effects (anodic current) are increased (a to d) and the overpotential for the oxidation of the Cys is decreased due to the advantage of the nanomaterials. The calibration curve was drawn based on amperometric currents versus different concentrations of CyS. The detection limit, linear range, and sensitivity of CyS were observed to be 18.5 nM, 50 nM–2.0 µM, and 10.19 $nAnM^{-1}$ cm^{-2}, respectively. In addition to the direct measurement of CyS, a variety of platforms is available that are immobilized with CyS and detected oxidative stress parameters (H_2O_2 or NO). Table 5 compares some more electrochemical sensors and biosensors

reported for the measurement of CyS [146-160] while a more comprehensive list is given in SI (Table S5).

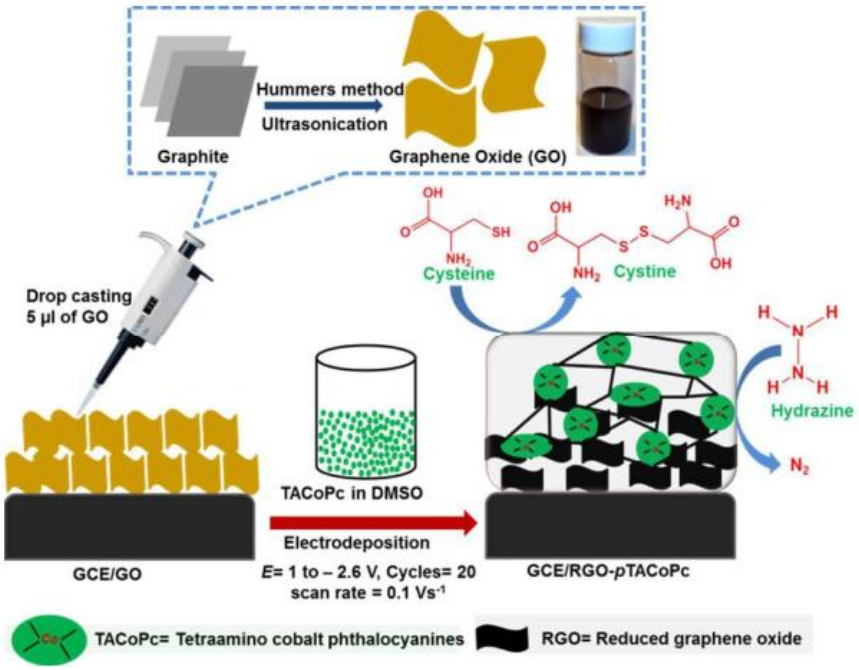

Fig. 18 Preparation of graphene oxide and electropolymerization of TACoPc on RGO for electrocatalytic determination of CyS and hydrazine [145].

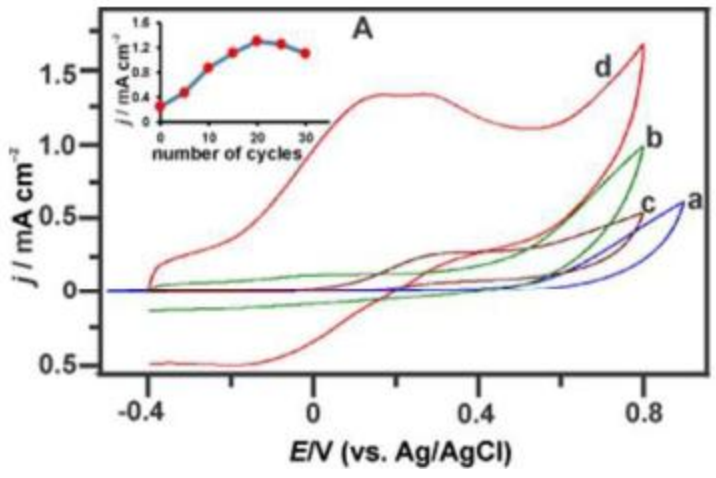

Fig. 19 cyclic voltammetry obtained at unmodified (a), RGO (b), pTACoPc (c) and RGO/pTACoPc composite (d) films modified electrodes in PB (pH= 7.0) containing 0.5 mM

CyS at scan rate 50 mVs^{-1}. Inset: optimization of cycle numbers for electrodeposition of pTACoPc at RGO/GCE [145].

Table 5. A comparison of some electrochemical sensing devices reported for cysteine, comparing factors such as the electrode, linear range, measurement method, and limit of detection.

Modified electrode	LOD (µM)	Linear range (µM)	method	Reference
AgSAE	0.003	0.01-0.2	CSDPV	[146]
GO–Au NCs/GC	0.02 M	0.05-20.0 M	CV	[147]
MnO_2-TiO_2/DPID/CPE	13	25–200000	SWV	[148]
MWCNT/CCLP-AuNPs/GCE	0.019	0.1-1,000	CV	[149]
p-APMCNTPE	0.3	0.5 – 100	DPV	[150]
CuGeO3-NW-GCE	9×10^{-7}	1×10^{-6} 1×10^{-3} M	CV	[151]
SPCE/PEDOT/AuNPs	0.05 M	0.5–200 M	DPV	[152]
GCE/CTC	0.6 mM	>40 mM	CV	[153]
Co^{2+}Y/ZMCPE	0.000237	0.001–1000	CV	[154]
AgNPs/GQDs/GCE	1×10^{-8} M	2×10^{-4} -1×10^{-7} M	DPV	[155]
Pt-Fe_3O_4/rGO/GCE	10	100-1000	DPV	[156]
GC/VO^{2+}-S	-	0.1-1.0 mM	LSV	[157]
FcFMSF/ITO	3	3- 20	AM	[158]
EFTAGCPE	0.9	4.0–2300.0	DPV	[159]
ZnTAPc-Gr	0.0114	0.25–113	PEC	[160]

AgSAE: silver solid amalgam electrode, CSDPV: cathodic strippring differential pulse voltammetry, CV: cyclic voltammetry, GO–Au NCs: graphene oxide/Au nanocluster, MnO_2: Magnesium oxide, TiO_2: titanium oxide, DPID: 2-(3,4 dihydroxyphenethyl) isoindoline-1,3-dione, CPE: carbon paste electrode, SWV: square wave voltammetry, p-APMCNTPE: p-aminophenol modified carbon nanotube paste electrode, DPV: differential pulse voltammetry, NW: nanowire, GCE: glassy carbon electrode, SPCE: screen-printed carbon electrode, PEDOT: poly(3,4-ethylenedioxythiophene, AuNPs: gold nanoparticles, CTC: cyclotricatechylene, Co^{2+}Y/ZM: Co(II)-exchanged zeolite Y, AgNPs/GQDs: silver nanoparticles/graphene quantum dots, Pt-Fe_3O_4/rGO/GCE: platinum, magnetite/reduced graphene oxide, CNF Carbon nanofibers, GC/VO^{2+}-S: glassy carbon/oxovanadium(IV) salen, LSV: linear scan voltammetry, FcFMSF: ferrocene-functionalised mesoporous silica films, ITO: indium-tin oxide, AM: amperometry, EFTAGCPE: ethyl 2-(4-ferrocenyl-[1,2,3]triazol-1-yl) acetate (EFTA) and graphene on carbon

paste electrode, ZnTAPc-Gr: zinc-tetramine phthalocyanine covalently grafted to graphene oxide, PEC: photoelectrochemical.

4.3. Methionine

Methionine (Met) is a thiol-containing antioxidant with low-molecular-weight, which participated in reducing cholesterol level, methylation processes, and protein production of the living system. Like the cysteine enzyme, the oxidation potential of Met is low and can be readily oxidized with ROS or RNS active species in vivo [161]. One of the analytical applications of Met is the usage of its polymer in the modification of electrodes for sensing pharmaceutical compounds and ions such as hypoxanthine uric acid, xanthine, tryptophan, dopamine, DL-methionine, and mercury(II) [162]. Bank et al. studied the electrochemical behavior of Met on boron-doped diamond electrode, and screen printed electrodes via differential pulse voltammetry [163]. The anodic oxidation signal was observed in the positive-going scan corresponding to the oxidation of sulfide into sulfone moities. Based on the early reports (slope of E vs. pH= −60 mV), the Met oxidation process occurs by losing four electrons and four protons at the electrode surface as illustrated in Fig. 20. Unfortunately, no stability data was provided for this sensor.

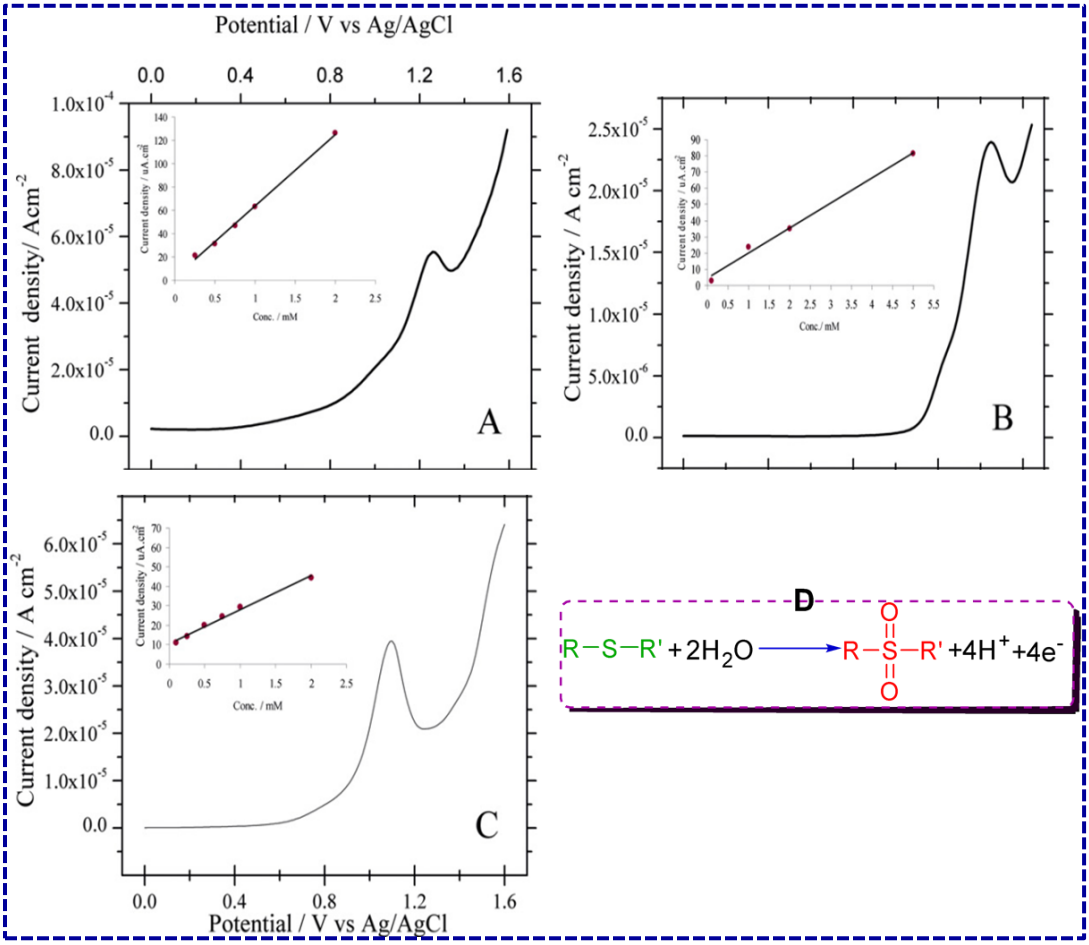

Fig. 20 DPV of different carbon-based electrodes: GC (A), BDD (B) and SPGE (C) for the direct oxidation of 1 mM Met in pH 7 0.1 M phosphate buffer solution. Insets: calibration plots for ranges between 0.25 and 2 mM for (A), 0.1 and 5 mM for (B), 0.1 and 2 mM for (C). (D) Oxidation pathway of Met [163].

Also, the overpotential of Met oxidation has been reduced on a variety of electrodes with the following order SPGE> BDD> GC at pH 7. The linear range and detection limit of 0.05–5.0 mM and 95 µM were obtained. Some electrochemical sensors for Met detection are presented in Table 6 and their electroanalytical parameters were compared [164-167]. (more comprehensive data can be found in Table S6 in SI).

Table 6 A comparison of electrochemical sensing devices for methionine, comparing factors such as the electrode, linear range, measurement method, and limit of detection.

Modified electrode	LOD (µM)	Linear range (µM)	Method	Reference
nAu-Cyst-CPE	0.59	1.0–100	DPV	[164]
GO/SPCE	0.18	2-96	CV	[165]
AuNP-GCE	$0.7x10^{-14}$ M	-	CV	[166]
AgO/GPE	0.42	60-500	LSV	[167]

nAu-Cyst-CPE: colloidal-gold cysteamine-modified carbon paste electrode, DPV: differential pulse voltammetry, GO/SPCE: graphene oxide/modified screen-printed carbon electrode, CV: cyclic voltammetry, AuNP-GCE: graphite electrode modified with gold nanoparticles, GPE: graphite pencil electrode, LSV: linear scan voltammetry.

4.4. Coenzyme Q

Coenzyme Q (CoQ_n) is a 2,3-dimethoxy-5- methyl-6-isoprenyl-1,4-benzoquinone derivative that the number of isoprene units (n) is ranging from zero to ten. Ubiquinone (oxidized CoQ_n), ubiquinol (reduced, CoQ_nH_2), and ubisemiquinone (semiquinone) are three types of CoQn redox states, and their concentrations in the biological and plasma matrices is depending on the presence or absence of ROS or RNS [168]. In other words, with the presence of iron-sulfur clusters in their structures, they scavenge the free radicals and change the redox state. As a consequence of biological function, CoQn derivatives exhibit prooxidative and antioxidant or anti-oxidative stress effects in living cells [169]. Diagnose and determination of the oxidized and reduced form of CoQ_n derivatives is significant for oxidative stress conditions and has a direct relationship with some other diseases such as Parkinson's, diabetes, hyperlipidemia, aging, and neonatal hypoxia [170]. Numerous studies were reported on the electrochemical behavior of CoQ_n derivatives in non-aqueous, aqueous, non-buffered, or buffered solutions, and observed that the number of oxidation and reduction peaks depends on protic or aprotic experiment media [171]. The most widely used endogenous coenzymes are CoQ10 that present in mammals and mitochondria. This enzyme has been analyzed in a variety of sample matrixes such as animal tissues, pharmaceutical, and biological samples using the simple electrochemical platforms (glassy carbon and Silver electrode) and electroanalytical methods (CV and DPV) in mixed

solvents. Recently, Barsan and Diculescu developed an electrochemical sensor to detect oxidative stress parameters (H_2O_2 and O_2^{2-}) on cyclodextrins (α-CD) + CoQ_{10}/Nafion modified GC electrode in H_2O_2 and KO_2 solution [172]. At constant oxidation or reduction potential, CoQ_{10} acts as a mediator for the conversion of ROS to inactive molecules, and the signal is detected using SWV and CA techniques, with good operational and storage stabilities (98% response kept after 5 successive measurements and ~90% after 2 months of storage at 4°C in air). The schematic of this approach is shown in Fig. 21. The comparative analytical parameters of some Coenzyme Q electrochemical sensors have been summarized in Table 7 [173-175] (with some more data in Table S7 in SI).

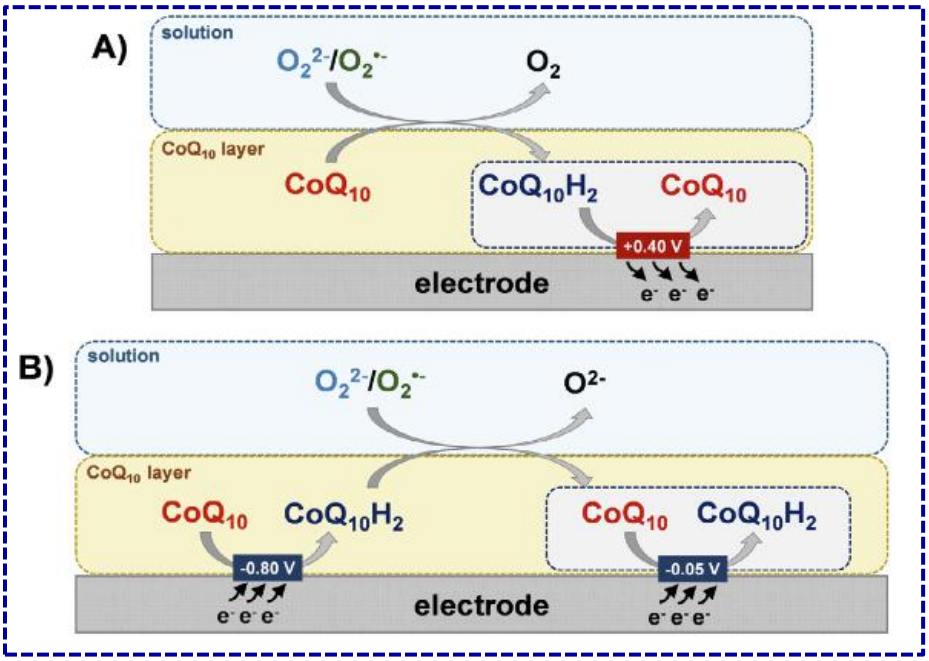

Fig. 21 Proposed electrochemical approaches to detection of oxidative stress parameters via $CoQ_{10}/CoQ_{10}H_2$ as a mediator and with A) chronoamperometry at positive potentials and B) SWV close to 0 V [172].

Table 7 A comparison of electrochemical sensing devices for coenzyme Q, comparing factors such as the electrode, linear range, measurement method, and limit of detection.

Modified electrode	**LOD (μM)**	**Linear range (μM)**	**Method**	**Reference**
Silver Electrode	0.0333	0.1 -1000	DPV	[173]
MnO_2/SPGE	0.56 μg mL^{-1}	2.0-75.0 μg mL^{-1}	SWASV	[174]
Microporous graphitic carbon	0.01	0.64-1.24 μg mL^{-1}	AM	[175]

DPV: differential pulse voltammetry, SPGE: screen-printed graphene electrode, SWASV: square wave anodic stripping voltammetry, AM: amperometry.

4.5. α- Lipoic acid

66,8-thioctic acid, 1,2-dithiolane-3-pentanoic acid, or α- Lipoic acid (LA) is an organosulfur compound and one of the most important molecules that have therapeutic potential in some organisms under conditions of injury or damage [176]. LA has a protective effect against ROS, RNS, or oxidative stress phenomenon and is known as vitamin-like. The antioxidant property of LA is due to the presence of a disulfide functional group in the LA structure, which is converted to β-Lipoic acid (BLA) in the presence of oxidizing species and is a biologically active substance [177]. As a result, the LA level can obtain by monitoring the oxidation of LA to BLA. Ziyatdinova et al. detected the LA using GCE via voltammetric methods [178] and obtained the detection limit of 5.75×10^{-6} M and the linear detection range of 1.15×10^{-5} to 1.73×10^{-4} M. In similar works, Fluorine-doped tin oxide electrode (FTO) [179], boron doped diamond (BDDE) [180], and pyrolytic graphite electrode modified (PG) with cobalt phthalocyanine (CoPc) (PG/CoPc) [181] have been used as a sensing platform for monitoring LA concentration in dietary supplements. The LODs of 3.68 µM, 3.4 nM, 4.07 µM, and 1.8 µM were obtained for FTO, PG/CoPc, Pt, and GCE, respectively, without however any available stability data.

In 2018, Sasikumar et al. reported electrochemical detection of LA using the functionalized multi-walled carbon nanotubes-polyindole/Ti_2O_3/GCE (*f*-MWCNTs-PIN/Ti_2O_3/GCE) [182]. The sensing electrode was prepared by the oxidation of MWCNT in HNO_3/H_2SO_4 solution, accumulation of MWCNT-COOH in $FeCl_2$, indole aqueous solution followed by ultrasonic, and autoclave treatments in 0.3g of titanium (III) oxide (Fig. 22).

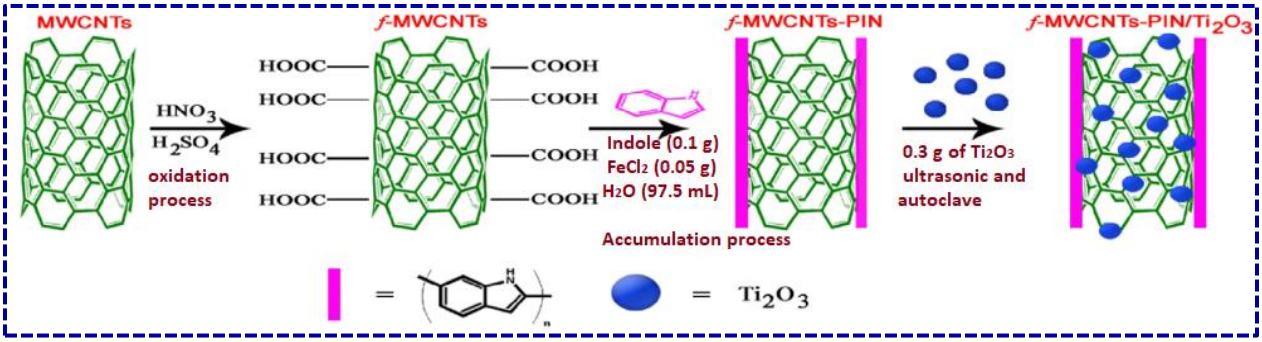

Fig. 22 The steps of *f*-MWCNTs-PIN/Ti_2O_3/GCE preparation for determination of LA [182].

The electrochemical activity of LA was pointed out for different electrodes via cyclic voltammetry in the positive-going scan. It can be seen from Fig. 23 that the maximum current has been detected on a functionalized multi-walled carbon nanotubes-polyindole/Ti_2O_3 nanocomposite modified glassy carbon electrode (f-MWCNTs-PIN/Ti_2O_3/GCE) in 0.05 M PBS

(pH 7), and the value of the detection limit is calculated to be 12 nM, with 95% storage stability for 2 weeks.

Recently, Ziyatdinova et al. presented a modified GCE based on cetyltriphenylphosphonium bromide (CTPPB) and SnO_2 nanoparticles with high surface area to obtain the detection limit of 0.13 and 0.43 μM and the linear range of 0.50–400 μM (Fig. 24) [183].

Lately, a carbon-fiber microelectrode has been used as a sensing platform, with a detection range between 0.25-123.2 mg L^{-1} and the LOD of 0.08 mg L^{-1} for the identification of LA in pharmaceutical preparations by Skorupa and Michalkiewicz [184].

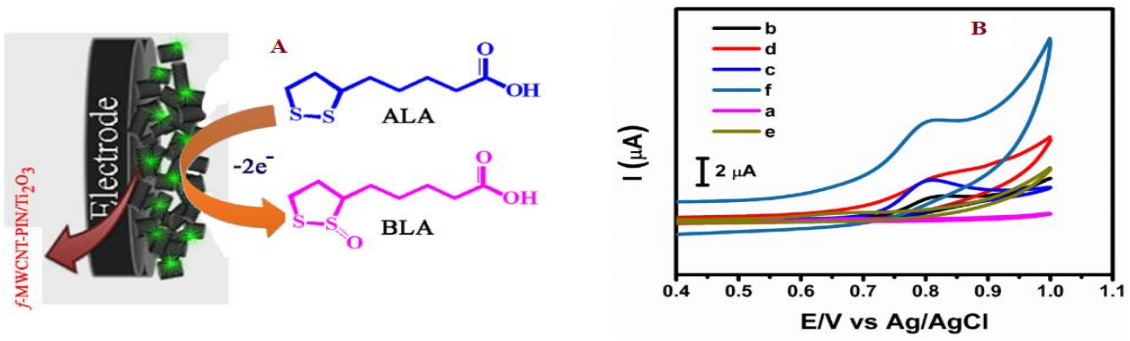

Fig. 23 (A) Oxidation mechanism of LA, (B) CVs of (a) bare GCE absence of ALA, (b) bare GCE presence of ALA, (c) fMWCNTs, (d) f-MWCNTs-PIN, (e) Ti_2O_3 (f) f-MWCNTs-PIN/Ti_2O_3/GCE with 200 μM ALA in 0.05 M PBS (pH 7). Scan rate: 50 mV s^{-1} [182].

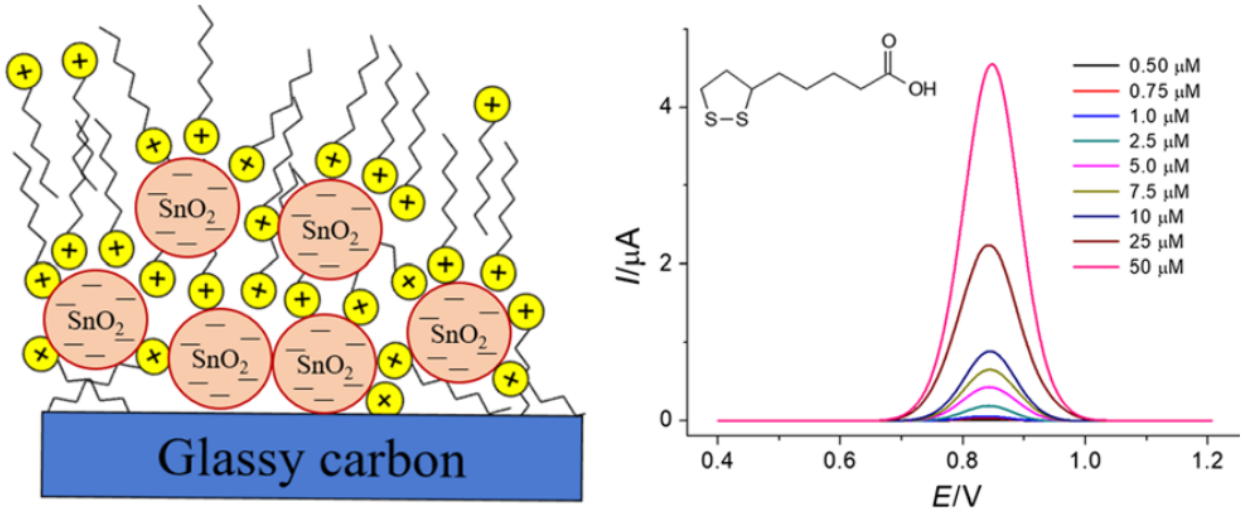

Fig. 24 Schematic representation for electrochemical detection of LA on SnO_2 NP-CTPPB/GCE [183].

4.6. Bilirubin

Bilirubin or hematoidin is a tetrapyrrole compound that is formed from two biological processes. First, the breakdown of heme in red blood cells, and second, the reduction of Biliverdin with bilirubin reductase. Iron deficiency and liver diseases are associated with low and high levels of bilirubin in the serum samples, respectively [185]. The anti-inflammatory [186] and antioxidant activities [187] of bilirubin were observed in the concentration range of 6 mg/dl to 12 mg/dl. In serum, the native (unconjugated) form of bilirubin is much lower than the conjugated form (with albumin) [188]); thus, the diagnostic of bilirubin as a marker of oxidative stress requires a sensitive method. Because of the electroactivity of this metabolite, the electrochemical approach can introduce a simple and fast procedure to measure bilirubin. In this way, enzymatic and non-enzymatic electrochemical sensors have been developed for the detection of bilirubin. In 2011, Kannan et al. constructed a sensitive platform based on the self-assembling of bilirubin oxidase (BOx) on gold nanoparticles (AuNPs) to determine the bilirubin concentration [189]. The (3-mercaptopropyl)-trimethoxysilane (MPTS) was used as an organosilane with thiol moiety to self-assemble AuNPs on the desired surface (Fig. 25). The amperometric technique at a constant potential (+0.35 V) was used to detect the bilirubin with a detection limit of 1.4 nM and the linear range 1-5000 M. Good stability and repeatability within a confidence level of 96% was obtained for 40 successive measurements, as well as appreciable long-term storage stability (identical response after two days small decrease by 3.4% after 10 days and 7% after more than 2 months). Table 8 offers a comparison of the analytical parameters reported for some electrochemical sensors for bilirubin detection [190-200] (with a more comprehensive Table S8 in SI).

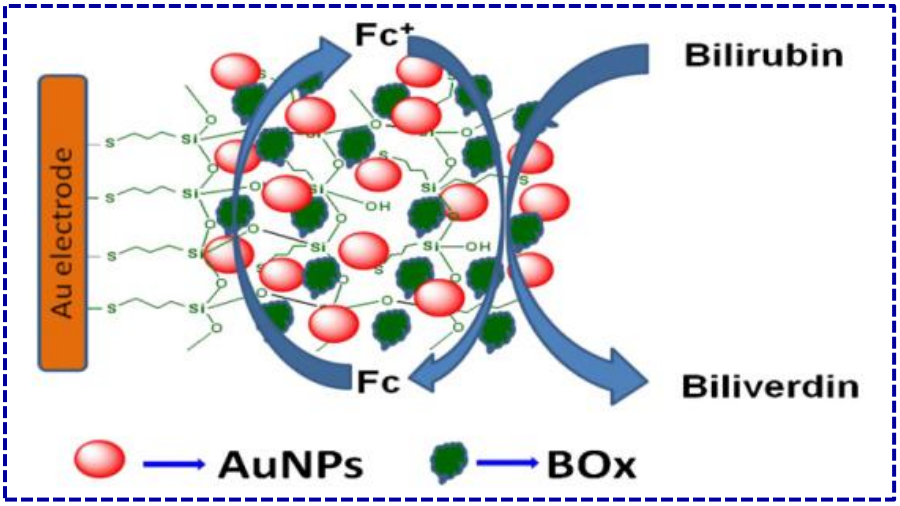

Fig. 25 Schematic representation of the oxidation of bilirubin occurred at Au/MPTS/AuNPs/BOx modified electrode [189].

Table 8 A comparison of electrochemical sensing devices for bilirubin, comparing factors such as the electrode, linear range, measurement method, and limit of detection.

Modified electrode	LOD (µM)	Linear range (µM)	Method	Reference
PVA/PAn-$NaZnPO_4$-AZO	1.2 µg/dl	0.05 µM–1.5 mM	PM	[190]
MIP/CNT/CPE	0.75	1-100	CV	[191]
DFM-CHIT-GCE	3300	10 nm to100 nM	CV	[192]
AuNPs/TTF-COOH/RGO	0.74	2.66-83	CV	[193]
ISE	0.1	0.10–1000	PM	[194]
Pt microelectrodes/CVD nanographite	56±33	----------	SWV	[195]
BOx/nano Au/CHIT/micro AuE	0.005	0.01 -500	EIS	[196]
Er-GR/SPE	0.1 ± 0.018	0.1–600	CV	[197]
MWCNT/SPE	0.3 ± 0.022	0.5–500	CV	[197]
CPE/ZnS NPs	2	3-50	CV	[198]
RM/MIPPy/QCM	0.003	0.01-120	EQCM	[199]
IAO-NRs/Nafion/GCE	16.5 ± 0.05 pM	0.1 nM - 0.01 M	I–V	[200]

PVA/PAn-$NaZnPO_4$-AZO: polyvinyl alcohol/polyaniline- sodium zinc phosphate-aluminum- doped zinc oxide, PM: potentiometry, MIP: molecularly imprinted polymer, CNT: carbon nanotube, CPE: carbon paste electrode, CV: cyclic voltammetry, DFM-CHIT: Diferuloylmethane-chitosan, GCE: glassy carbon electrode, AuNPs/TTF-COOH/RGO: Au nanoparticles/ tetrathiafulvalene-carboxylate functionalized reduced graphene oxide, ISE: ion selective electrode, SWV: square wave voltammetry, BOx/nano Au: bilirubin oxidase on gold nanorods, CHIT: chitosan, EIS: electrochemical impedance spectroscopy, Er-GR: electrochemically reduced graphene oxide, SPE: screnn-printed electrode, MWCNT: multiwall carbon nanotube, ZnS NPs: ZnS nanoparticles, RM/MIPPy: Red mud/molecularly imprinted polypyrrole, EQCM: electrochemical quartz crystal microbalance, IAO-NRs: iron-doped antimony oxide nanorods.

5. Conclusion and outlook

In summary, this review details the electrochemical sensors and biosensors reported for measuring the oxidative stress biomarkers. Different recognition and biorecognition elements were used while preparing the electrode design for sensing. The role of the various micro and nanomaterials used as electrode modifiers is mostly to enhance the electrocatalytic activity or diagnostic sensitivity by increasing the surface area and/or facilitating electron transfer between

the electrode and the analyte so that the tiny amount of oxidative stress biomarkers can be determined. The concentration of the analyte (biomarkers and antioxidant agents) is assessed by monitoring the biosensor/sensor output electrochemical signals before/after binding to the analyte. Designing commercial diagnostic kits for oxidative stress biomarkers either as directly (detection of biomarkers) or indirectly (monitoring of antioxidant status) can be of considerable help to biomedical labs, and diagnostic clinics to monitor the biological systems. The electrochemical approach is an inexpensive, quantitative, and accurate analytical tool for the early detection of oxidative stress biomarkers in-vivo and in-vitro media.

Several commercial oxidative stress assay kits such as catalase, xanthine oxidase, hydrogen peroxide (H_2O_2), myeloperoxidase human environmental impact assessment (EIA), superoxide dismutase (SOD), myeloperoxidase (MPO), glutathione reductase (GR) activity, and DNA damage EIA, FRAP, glutathione, nitric oxide (NO_2^-/NO_3^-), thiol fluorescent, lipid peroxidation (MDA), ascorbic acid, protein carbonyl, uric acid, and formaldehyde content detection are commercially available in the market and are mainly colorimetric and fluorometric tests. Electrochemical biosensors/sensors developed so far have substantial potential to startup a commercial oxidative stress kit, and have the potential to be a billion-dollar market, while the technology (chemical and electrochemical) requires further improvement in signal transduction, biological stability, accuracy, and cost-effectiveness. The following important points must be considered in near future to transform the laboratory sensing device to the market scale. 1) The electrode modification process must be fewer steps. 2) Development of innovative, low-cost, and more specific procedures for the synthesis of specific recognition materials and functionalization of electrodes needed. The transduction of the recognition events into a readable signal must be optimized to perform the sensing with high reproducibility and reliability. 3) Advanced inter-sector such as electrochemistry, biochemistry, biotechnology, biology, and biomedical science, electronics engineering, etc. tie-up is required to launch successful oxidative stress sensors and biosensors commercial electronic kits. 4). We believe that future signal transducers could be designed by immobilizing several biorecognition elements (antibody, aptamer, etc.) and be used in the simultaneous detection of several biomarkers.

Conflict of interest

There is no conflict of interest among the authors.

Acknowledgments

We acknowledge the Hamedan University of Medical Sciences, Research and Technology Vice-Chancellor (grant number: 980210464).

Supplementary Information

Extensive Tables (S1-S8) describing the electrode configuration and analytical performance of sensors and biosensors for myeloperoxidase, lipoprotein, 8-hydroxydeoxyguanosine, glutathione, cysteine, methionine, coenzyme Q and bilirubin, with a list of the corresponding cited references at the end.

References

1. Abdollahi M, Ranjbar A, Shadnia S, Nikfar S, Rezaiee A (2004) Pesticides and oxidative stress: a review. Medical Science Monitor 10(6):RA141-RA147

2. Halliwell B, Gutteridge JM (2015) Free radicals in biology and medicine. Oxford University Press, USA

3. Bansal M, Kaushal N (2014) Oxidative stress mechanisms and their modulation. Springer

4. Ranjbar A, Solhi H, Mashayekhi FJ, Susanabdi A, Rezaie A, Abdollahi M (2005) Oxidative stress in acute human poisoning with organophosphorus insecticides; a case control study. Environmental toxicology and pharmacology 20(1):88-91

5. Liguori I, Russo G, Curcio F, Bulli G, Aran L, Della-Morte D, Gargiulo G, Testa G, Cacciatore F, Bonaduce D (2018) Oxidative stress, aging, and diseases. Clinical interventions in aging 13:757

6. Maheshwaran S, Akilarasan M, Chen S-M, Chen T-W, Tamilalagan E, Tzu CY, Lou B-S (2020) An ultra-sensitive electrochemical sensor for the detection of oxidative stress biomarker 3-nitro-l-tyrosine in human blood serum and saliva samples based on reduced graphene oxide entrapped zirconium (IV) oxide. Journal of The Electrochemical Society 167(6):066517

7. Enache TA, Matei E, Diculescu VC (2018) Electrochemical sensor for carbonyl groups in oxidized proteins. Analytical chemistry 91(3):1920-1927

8. Niki E (2008) Lipid peroxidation products as oxidative stress biomarkers. Biofactors 34(2):171-180

9. Frijhoff J, Winyard PG, Zarkovic N, Davies SS, Stocker R, Cheng D, Knight AR, Taylor EL, Oettrich J, Ruskovska T (2015) Clinical relevance of biomarkers of oxidative stress. Antioxidants & redox signaling 23(14):1144-1170

10. Ho E, Galougahi KK, Liu C-C, Bhindi R, Figtree GA (2013) Biological markers of oxidative stress: applications to cardiovascular research and practice. Redox biology 1(1):483-491

11. Ammanath G, Yildiz UH, Palaniappan A, Liedberg B (2018) Luminescent device for the detection of oxidative stress biomarkers in artificial urine. ACS applied materials & interfaces 10(9):7730-7736

12. Kopáni M, Celec P, Danišovič L, Michalka P, Biró C (2006) Oxidative stress and electron spin resonance. Clinica chimica acta 364(1-2):61-66

13. Zhang Z, Liu Q, Liu Y, Qi R, Zhou L, Li Z, Yun J, Liu R, Hu Y (2020) Colorimetric H2O2 Detection Using Ag-Nanoparticle-Decorated Silica Microspheres. Nano 15(01):2050009

14. Wei L, Lu X, Kang X, Song Y (2020) Determination of Glutathione and Cysteine in Human Breast Milk by High-Performance Liquid Chromatography with Chemiluminescence Detection for Evaluating the Oxidative Stress and Exposure to Heavy Metals of Lactating Women. Analytical Letters 53(16):2607-2618

15. Stryjak I, Warmuzińska N, Bogusiewicz J, Łuczykowski K, Bojko B (2020) Monitoring of the influence of long- term oxidative stress and ischemia on the condition of kidneys using solid- phase microextraction chemical biopsy coupled with liquid chromatography–high- resolution mass spectrometry. Journal of separation science 43(9-10):1867-1878

16. Liang C, Chen X, Tang Q, Ji W, Jiang Y, Mao L, Wang M (2020) An activity-based two-photon fluorescent probe for real-time and reversible imaging of oxidative stress in the rat brain. Chemical Communications 56(47):6368-6371

17. Zhu Y, Wu J, Wang K, Xu H, Qu M, Gao Z, Guo L, Xie J (2021) Facile and sensitive measurement of GSH/GSSG in cells by surface-enhanced Raman spectroscopy. Talanta 224:121852

18. Ostojić J, Herenda S, Bešić Z, Miloš M, Galić B (2017) Advantages of an electrochemical method compared to the spectrophotometric kinetic study of peroxidase inhibition by boroxine derivative. Molecules 22(7):1120

19. Numal R, Selcuk O, Kurbanoglu S, Shah A, Siddiq M, Uslu B (2022) Trends In Electrochemical Nanosensors For The Analysis Of Antioxidants. TrAC Trends in Analytical Chemistry:116626

20. Rojas D, Hernández-Rodríguez JF, Della Pelle F, Escarpa A, Compagnone D (2022) New trends in enzyme-free electrochemical sensing of ROS/RNS. Application to live cell analysis. Microchimica Acta 189(3):1-22

21. Amatore C, Arbault S, Guille M, Lemaitre F (2008) Electrochemical monitoring of single cell secretion: vesicular exocytosis and oxidative stress. Chemical reviews 108(7):2585-2621

22. Brainina KZ, Shpigun LK (2022) State- of- the- art electrochemistry for the assessment of oxidative stress and integral antioxidant activity of biological environments. Electrochemical Science Advances:e2100219

23. Ahoulou S, Vilà N, Pillet S, Schaniel D, Walcarius A (2020) Non- covalent Immobilization of Iron- triazole (Fe (Htrz) 3) Molecular Mediator in Mesoporous Silica Films for the Electrochemical Detection of Hydrogen Peroxide. Electroanalysis 32(4):690-697

24. Balamurugan M, Santharaman P, Madasamy T, Rajesh S, Sethy NK, Bhargava K, Kotamraju S, Karunakaran C (2018) Recent trends in electrochemical biosensors of superoxide dismutases. Biosensors and Bioelectronics 116:89-99

25. Khan AA, Alsahli MA, Rahmani AH (2018) Myeloperoxidase as an active disease biomarker: recent biochemical and pathological perspectives. Medical Sciences 6(2):33

26. Nakazato T, Sagawa M, Yamato K, Xian M, Yamamoto T, Suematsu M, Ikeda Y, Kizaki M (2007) Myeloperoxidase is a key regulator of oxidative stress–mediated apoptosis in myeloid leukemic cells. Clinical Cancer Research 13(18):5436-5445

27. Nybo T, Cai H, Chuang CY, Gamon LF, Rogowska-Wrzesinska A, Davies MJ (2018) Chlorination and oxidation of human plasma fibronectin by myeloperoxidase-derived oxidants, and its consequences for smooth muscle cell function. Redox biology 19:388-400

28. Ndrepepa G (2019) Myeloperoxidase–A bridge linking inflammation and oxidative stress with cardiovascular disease. Clin Chim Acta

29. Koeth RA, Haselden V, Tang WW (2013) Myeloperoxidase in cardiovascular disease. Advances in clinical chemistry. Elsevier, pp 1-32

30. Chandler JD, Margaroli C, Horati H, Kilgore MB, Veltman M, Liu HK, Taurone AJ, Peng L, Guglani L, Uppal K (2018) Myeloperoxidase oxidation of methionine associates with early cystic fibrosis lung disease. European Respiratory Journal 52(4)

31. Liu B, Lu L (2019) Amperometric sandwich immunoassay for determination of myeloperoxidase by using gold nanoparticles encapsulated in graphitized mesoporous carbon. Microchimica Acta 186(4):262

32. Bekhit M, Gorski W (2019) Electrochemical Assays and Immunoassays of the Myeloperoxidase/SCN–/H2O2 System. Anal Chem 91(4):3163-3169

33. Barallat J, Olivé-Monllau R, Gonzalo-Ruiz J, Ramírez-Satorras Rl, Muñoz-Pascual FX, Ortega AGn, Baldrich E (2013) Chronoamperometric magneto immunosensor for myeloperoxidase detection in human plasma based on a magnetic switch produced by 3D laser sintering. Anal Chem 85(19):9049-9056

34. Diao QZ, Li Y, Zhou M, Xie GM (2012) A new immunosensor for serum myeloperoxidase based on self-assembly of multi-walled carbon nanotubes/thionine/gold nanoparticles-chitosan. In: Advanced Materials Research. Trans Tech Publ, pp 1207-1211

35. Lu L, Liu B, Li S, Zhang W, Xie G (2011) Improved electrochemical immunosensor for myeloperoxidase in human serum based on nanogold/cerium dioxide-BMIMPF6/l-Cysteine composite film. Colloids and Surfaces B: Biointerfaces 86(2):339-344

36. Panday A, Sahoo MK, Osorio D, Batra S (2015) NADPH oxidases: an overview from structure to innate immunity-associated pathologies. Cellular & molecular immunology 12(1):5-23

37. Atashi F, Modarressi A, Pepper MS (2015) The role of reactive oxygen species in mesenchymal stem cell adipogenic and osteogenic differentiation: a review. Stem cells and development 24(10):1150-1163

38. Drummond GR, Selemidis S, Griendling KK, Sobey CG (2011) Combating oxidative stress in vascular disease: NADPH oxidases as therapeutic targets. Nature reviews Drug discovery 10(6):453-471

39. Shimohama S, Tanino H, Kawakami N, Okamura N, Kodama H, Yamaguchi T, Hayakawa T, Nunomura A, Chiba S, Perry G (2000) Activation of NADPH oxidase in Alzheimer's disease brains. Biochem Biophys Res Commun 273(1):5-9

40. Sekioka N, Kato D, Kurita R, Hirono S, Niwa O (2008) Improved detection limit for an electrochemical γ-aminobutyric acid sensor based on stable NADPH detection using an electron cyclotron resonance sputtered carbon film electrode. Sensors and Actuators B: Chemical 129(1):442-449

41. Ashkenazi A, Abu-Rabeah K, Marks R (2009) Electrochemistry and chemiluminescence techniques compared in the detection of NADPH oxidase activity in phagocyte cells. Talanta 77(4):1460-1465

42. Ghosh C, Hossain M, Solanki J, Dadas A, Marchi N, Janigro D (2016) Pathophysiological implications of neurovascular P450 in brain disorders. Drug Discovery Today 21(10):1609-1619

43. Fleming BD, Tian Y, Bell SG, Wong LL, Urlacher V, Hill HAO (2003) Redox properties of cytochrome P450BM3 measured by direct methods. Eur J Biochem 270(20):4082-4088

44. Fantuzzi A, Fairhead M, Gilardi G (2004) Direct electrochemistry of immobilized human cytochrome P450 2E1. J Am Chem Soc 126(16):5040-5041

45. Peng L, Yang X, Zhang Q, Liu S (2008) Electrochemistry of cytochrome P450 2B6 on electrodes modified with zirconium dioxide nanoparticles and platin components. Electroanalysis: An International Journal Devoted to Fundamental and Practical Aspects of Electroanalysis 20(7):803-807

46. Rhieu SY, Ludwig DR, Siu VS, Palmore GTR (2009) Direct electrochemistry of cytochrome P450 27B1 in surfactant films. Electrochem Commun 11(10):1857-1860

47. Shumyantseva VV, Carrara S, Bavastrello V, Riley DJ, Bulko TV, Skryabin KG, Archakov AI, Nicolini C (2005) Direct electron transfer between cytochrome P450scc and gold nanoparticles on screen-printed rhodium–graphite electrodes. Biosensors and Bioelectronics 21(1):217-222

48. Baj-Rossi C, Jost TR, Cavallini A, Grassi F, De Micheli G, Carrara S (2014) Continuous monitoring of Naproxen by a cytochrome P450-based electrochemical sensor. Biosensors and Bioelectronics 53:283-287

49. Müller M, Agarwal N, Kim J (2016) A cytochrome P450 3A4 biosensor based on generation 4.0 PAMAM dendrimers for the detection of caffeine. Biosensors 6(3):44

50. Tiwari BK, Pandey KB, Abidi A, Rizvi SI (2013) Markers of oxidative stress during diabetes mellitus. Journal of biomarkers 2013

51. Armenteros M, Heinonen M, Ollilainen V, Toldrá F, Estevez M (2009) Analysis of protein carbonyls in meat products by using the DNPH-method, fluorescence spectroscopy and liquid chromatography–electrospray ionisation–mass spectrometry (LC–ESI–MS). Meat Science 83(1):104-112

52. Marrocco I, Altieri F, Peluso I (2017) Measurement and clinical significance of biomarkers of oxidative stress in humans. Oxidative medicine and cellular longevity 2017

53. Boumya W, Hammani H, Laghrib F, Lahrich S, Farahi A, Achak M, Bakasse M, Mhammedi ME (2017) Electrochemical Study of 2, 4- Dinitrophenylhydrazine as Derivatization Reagent and Aldehydes at Carbon Glassy Electrode. Electroanalysis 29(7):1700-1711

54. Saczk A, Okumura L, De Oliveira M, Zanoni MVB, Stradiotto NR (2006) Determination of aldehydes and ketones in fuel ethanol by high-performance liquid chromatography with electrochemical detection. Chromatographia 63(1-2):45-51

55. Ferrer-Sueta G, Campolo N, Trujillo M, Bartesaghi S, Carballal Sn, Romero N, Alvarez B, Radi R (2018) Biochemistry of peroxynitrite and protein tyrosine nitration. Chem Rev 118(3):1338-1408

56. Castegna A, Thongboonkerd V, Klein JB, Lynn B, Markesbery WR, Butterfield DA (2003) Proteomic identification of nitrated proteins in Alzheimer's disease brain. J Neurochem 85(6):1394-1401

57. Hensley K, Williamson KS, Floyd RA (2000) Measurement of 3-nitrotyrosine and 5-nitro-γ-tocopherol by high-performance liquid chromatography with electrochemical detection. Free Radical Biol Med 28(4):520-528

58. Ali HM, Alsohaimi IH, Nayl A, Essawy AA, Gamal M, Ibrahim H (2022) A new ultrasensitive platform based on f-GCNFs@ nano-CeO2 core-shell nanocomposite for electrochemical sensing of oxidative stress biomarker 3-nitrotyrosine in presence of uric acid and tyrosine. Microchemical Journal:108068

59. Bandookwala M, Thakkar D, Sengupta P (2020) Advancements in the analytical quantification of nitroxidative stress biomarker 3-nitrotyrosine in biological matrices. Crit Rev Anal Chem 50(3):265-289

60. Zhang Y, Yang H, Pöschl U (2011) Analysis of nitrated proteins and tryptic peptides by HPLC-chip-MS/MS: site-specific quantification, nitration degree, and reactivity of tyrosine residues. Anal Bioanal Chem 399(1):459-471

61. Chen H-JC, Chiu W-L (2008) Simultaneous detection and quantification of 3-nitrotyrosine and 3-bromotyrosine in human urine by stable isotope dilution liquid chromatography tandem mass spectrometry. Toxicol Lett 181(1):31-39

62. Martins GV, Marques AC, Fortunato E, Sales MGF (2018) Wax-printed paper-based device for direct electrochemical detection of 3-nitrotyrosine. Electrochim Acta 284:60-68

63. Roy E, Patra S, Madhuri R, Sharma PK (2015) Developing electrochemical sensor for point-of-care diagnostics of oxidative stress marker using imprinted bimetallic Fe/Pd nanoparticle. Talanta 132:406-415

64. Wang S, Sun G, Chen Z, Liang Y, Zhou Q, Pan Y, Zhai H (2018) Constructing a novel composite of molecularly imprinted polymer-coated AuNPs electrochemical sensor for the determination of 3-nitrotyrosine. Electrochim Acta 259:893-902

65. Richards DA, Silva MA, Devall AJ (2006) Electrochemical detection of free 3-nitrotyrosine: application to microdialysis studies. Anal Biochem 351(1):77-83

66. Itabe H (2012) Oxidized low-density lipoprotein as a biomarker of in vivo oxidative stress: from atherosclerosis to periodontitis. Journal of clinical biochemistry and nutrition 51(1):1-8

67. Hirowatari Y, Yoshida H (2019) Innovatively Established Analysis Method for Lipoprotein Profiles Based on High-Performance Anion-Exchange Liquid Chromatography. Journal of atherosclerosis and thrombosis:RV17037

68. Ali MA, Singh N, Srivastava S, Agrawal VV, John R, Onoda M, Malhotra BD (2014) Chitosan-modified carbon nanotubes-based platform for low-density lipoprotein detection. Appl Biochem Biotechnol 174(3):926-935

69. Matharu Z, Sumana G, Gupta V, Malhotra B (2010) Langmuir–Blodgett films of polyaniline for low density lipoprotein detection. Thin Solid Films 519(3):1110-1114

70. Yan W, Chen X, Li X, Feng X, Zhu J-J (2008) Fabrication of a label-free electrochemical immunosensor of low-density lipoprotein. The Journal of Physical Chemistry B 112(4):1275-1281

71. Kaur G, Tomar M, Gupta V (2017) Nanostructured NiO-based reagentless biosensor for total cholesterol and low density lipoprotein detection. Anal Bioanal Chem 409(8):1995-2005

72. Oliveira MD, Abdalla DS, Guilherme DF, Faulin TE, Andrade CA (2011) Impedimetric immunosensor for electronegative low density lipoprotein (LDL−) based on monoclonal

antibody adsorbed on (polyvinyl formal)–gold nanoparticles matrix. Sensors and Actuators B: Chemical 155(2):775-781

73. Cabral-Miranda G, Yamashiro-Kanashiro E, Gidlund M, Sales MGF (2014) Specific label-free and real-time detection of oxidized low density lipoprotein (oxLDL) using an immunosensor with three monoclonal antibodies. Journal of Materials Chemistry B 2(5):477-484

74. Kaur G, Tomar M, Gupta V (2016) Realization of a label-free electrochemical immunosensor for detection of low density lipoprotein using NiO thin film. Biosensors and Bioelectronics 80:294-299

75. Chen J, Zeng L, Xia T, Li S, Yan T, Wu S, Qiu G, Liu Z (2015) Toward a biomarker of oxidative stress: a fluorescent probe for exogenous and endogenous malondialdehyde in living cells. Anal Chem 87(16):8052-8056

76. Khan MA, Baseer A (2000) Increased malondialdehyde levels in coronary heart disease. J Pak Med Assoc 50(8):261-264

77. Zhang G, Tang Y, Shi X, Gao R, Sun Y, Du W, Fu Q (2013) A chemiluminescence method to detect malondialdehyde in plasma and urine. Anal Biochem 443(1):16-21

78. Zhang D, Haputhanthri R, Ansar SM, Vangala K, De Silva HI, Sygula A, Saebo S, Pittman CU (2010) Ultrasensitive detection of malondialdehyde with surface-enhanced Raman spectroscopy. Anal Bioanal Chem 398(7-8):3193-3201

79. Stalikas CD, Konidari CN (2001) Analysis of malondialdehyde in biological matrices by capillary gas chromatography with electron-capture detection and mass spectrometry. Anal Biochem 290(1):108-115

80. Yuan L, Lan Y, Han M, Bao J, Tu W, Dai Z (2013) Label-free and facile electrochemical biosensing using carbon nanotubes for malondialdehyde detection. Analyst 138(11):3131-3134

81. Hasanzadeh M, Mokhtari F, Jouyban- Gharamaleki V, Mokhtarzadeh A, Shadjou N (2018) Electrochemical monitoring of malondialdehyde biomarker in biological samples via electropolymerized amino acid/chitosan nanocomposite. Journal of Molecular Recognition 31(8):e2717

82. Bhat LR, Vedantham S, Krishnan UM, Rayappan JBB (2019) Methylglyoxal–an emerging biomarker for diabetes mellitus diagnosis and its detection methods. Biosensors and bioelectronics

83. Kalapos MP, Desai KM, Wu L (2010) Methylglyoxal, oxidative stress, and aging. Aging and Age-Related Disorders. Springer, pp 149-167

84. Dhananjayan K, Irrgang F, Raju R, Harman DG, Moran C, Srikanth V, Münch G (2019) Determination of glyoxal and methylglyoxal in serum by UHPLC coupled with fluorescence detection. Anal Biochem 573:51-66

85. Wu X, Zhang W, Morales-Verdejo C, Sheng Y, Camarada MB, Chen L, Huang Z, Wen Y (2019) Nanohybrid sensor for simple, cheap, and sensitive electrochemical recognition and detection of methylglyoxal as chemical markers. Journal of Electroanalytical Chemistry 839:177-186

86. Chatterjee S, Wen J, Chen A (2013) Electrochemical determination of methylglyoxal as a biomarker in humanplasma. Biosensors and Bioelectronics 42:349-354

87. Jayaprakasan A, Thangavel A, Bhat LR, Gumpu MB, Nesakumar N, Babu KJ, Vedantham S, Rayappan JBB (2018) Fabrication of an electrochemical biosensor with ZnO nanoflakes interface for methylglyoxal quantification in food samples. Food science and biotechnology 27(1):9-17

88. Alagappan LP, Shanmugasundaram P, Ramachandra BL, Gumpu MB, Nesakumar N, Babu KJ, Vedantham S, Rayappan JBB (2017) Fabrication of electrochemical biosensor with vanadium pentoxide nano-interface for the detection of methylglyoxal in rice. Anal Biochem 528:19-25

89. Ramachandra BL, Vedantham S, Krishnan UM, Nesakumar N, Rayappan JBB (2016) Estimation of methylglyoxal in cow milk–an accurate electrochemical response time based approach. Analytical methods 8(10):2207-2217

90. Spickett CM (2013) The lipid peroxidation product 4-hydroxy-2-nonenal: advances in chemistry and analysis. Redox biology 1(1):145-152

91. Schaur RJ, Siems W, Bresgen N, Eckl PM (2015) 4-Hydroxy-nonenal—a bioactive lipid peroxidation product. Biomolecules 5(4):2247-2337

92. Goldring C, Casini AF, Maellaro E, Del Bello B, Comporti M (1993) Determination of 4-hydroxynonenal by high-performance liquid chromatography with electrochemical detection. Lipids 28(2):141-145

93. Luo J, Shi R (2005) Acrolein induces oxidative stress in brain mitochondria. Neurochem Int 46(3):243-252

94. Casella IG, Gatta M (2002) Determination of aliphatic organic acids by high-performance liquid chromatography with pulsed electrochemical detection. J Agric Food Chem 50(1):23-28

95. Dossi N, Susmel S, Toniolo R, Pizzariello A, Bontempelli G (2009) Application of microchip electrophoresis with electrochemical detection to environmental aldehyde monitoring. Electrophoresis 30(19):3465-3471

96. Montuschi P, Barnes PJ, Roberts LJ (2004) Isoprostanes: markers and mediators of oxidative stress. The FASEB Journal 18(15):1791-1800

97. Psathakis K, Papatheodorou G, Plataki M, Panagou P, Loukides S, Siafakas NM, Bouros D (2004) 8-Isoprostane, a marker of oxidative stress, is increased in the expired breath condensate of patients with pulmonary sarcoidosis. Chest 125(3):1005-1011

98. Peña-Bautista C, Baquero M, López-Nogueroles M, Vento M, Hervás D, Cháfer-Pericás C (2020) Isoprostanoids Levels in Cerebrospinal Fluid Do Not Reflect Alzheimer's Disease. Antioxidants 9(5):407

99. Sánchez-Tirado E, González-Cortés A, Yudasaka M, Iijima S, Langa F, Yáñez-Sedeño P, Pingarrón J (2017) Electrochemical immunosensor for the determination of 8-isoprostane aging biomarker using carbon nanohorns-modified disposable electrodes. Journal of Electroanalytical Chemistry 793:197-202

100. Lee G, Lee J, Kim J, Choi HS, Kim J, Lee S, Lee H (2017) Single microfluidic electrochemical sensor system for simultaneous multi-pulmonary hypertension biomarker analyses. Scientific reports 7(1):1-8

101. Tsai M-C, Huang T-L (2015) Thiobarbituric acid reactive substances (TBARS) is a state biomarker of oxidative stress in bipolar patients in a manic phase. Journal of affective disorders 173:22-26

102. Vaneesorn Y, Smyth WF (1980) The determination of some 2-thiobarbiturates by cathodic stripping voltammetry. Analytica Chimica Acta 117:183-191

103. Shahrokhian S, Hamzehloei A, Thaghani A, Mousavi SR (2004) Electrocatalytic Oxidation of 2- Thiouracil and 2- Thiobarbituric Acid at a Carbon- Paste Electrode Modified with Cobalt Phthalocyanine. Electroanalysis: An International Journal Devoted to Fundamental and Practical Aspects of Electroanalysis 16(11):915-921

104. You T, Yang X, Wang E (2000) Determination of barbituric acid and 2-thiobarbituric acid with end-column electrochemical detection by capillary electrophoresis. Talanta 51(6):1213-1218

105. Zhang D, Zhang J, Li M, Li W, Aimaiti G, Tuersun G, Ye J, Chu Q (2011) A novel miniaturised electrophoretic method for determining formaldehyde and acetaldehyde in food using 2-thiobarbituric acid derivatisation. Food Chem 129(1):206-212

106. Nishida N, Arizumi T, Takita M, Kitai S, Yada N, Hagiwara S, Inoue T, Minami Y, Ueshima K, Sakurai T (2013) Reactive oxygen species induce epigenetic instability through the formation of 8-hydroxydeoxyguanosine in human hepatocarcinogenesis. Digestive Diseases 31(5-6):459-466

107. Wu LL, Chiou C-C, Chang P-Y, Wu JT (2004) Urinary 8-OHdG: a marker of oxidative stress to DNA and a risk factor for cancer, atherosclerosis and diabetics. Clinica chimica acta 339(1-2):1-9

108. Chiorcea-Paquim A-M (2022) 8-oxoguanine and 8-oxodeoxyguanosine Biomarkers of Oxidative DNA Damage: A Review on HPLC–ECD Determination. Molecules 27(5):1620

109. Lin R, Zhou S, Zhao H, Lin H, Wang L, Hu W, Gao H, Qiu B (2022) A novel signal enhancement strategy for the detection of DNA oxidative damage biomarker 8-OHdG based on the synergy between β-CD-CuNCs and multi-walled carbon nanotubes. American Journal of Translational Research 14(2):740

110. Gutiérrez A, Gutiérrez S, García G, Galicia L, Rivas GA (2011) Determinatiom of 8- Hydroxy 2′- Deoxyguanosine Using Electrodes Modified with a Dispersion of Carbon Nanotubes in Polyethylenimine. Electroanalysis 23(5):1221-1228

111. Govindasamy M, Wang S-F, Subramanian B, Ramalingam RJ, Al-Lohedan H, Sathiyan A (2019) A novel electrochemical sensor for determination of DNA damage biomarker (8-hydroxy-2′-deoxyguanosine) in urine using sonochemically derived graphene oxide sheets covered zinc oxide flower modified electrode. Ultrason Sonochem 58:104622

112. Yang L, Wang B, Qi H, Gao Q, Li C-z, Zhang C (2015) Highly sensitive electrochemical sensor for the determination of 8-hydroxy-2′-deoxyguanosine incorporating SWCNTs-Nafion composite film. Journal of Sensors 2015

113. Khan M, Liu X, Tang Y, Liu X (2018) Ultra-sensitive electrochemical detection of oxidative stress biomarker 8-hydroxy-2′-deoxyguanosine with poly (L-arginine)/graphene wrapped Au nanoparticles modified electrode. Biosensors and Bioelectronics 117:508-514

114. Jia L-P, Liu J-F, Wang H-S (2015) Electrochemical performance and detection of 8-Hydroxy-2′-deoxyguanosine at single-stranded DNA functionalized graphene modified glassy carbon electrode. Biosensors and Bioelectronics 67:139-145

115. Martins GV, Tavares AP, Fortunato E, Sales MGF (2017) based sensing device for electrochemical detection of oxidative stress biomarker 8-hydroxy-2′-deoxyguanosine (8-OHdG) in point-of-care. Scientific reports 7(1):1-10

116. Pan D, Zhou Q, Rong S, Zhang G, Zhang Y, Liu F, Li M, Chang D, Pan H (2016) Electrochemical immunoassay for the biomarker 8-hydroxy-2′-deoxyguanosine using a glassy carbon electrode modified with chitosan and poly (indole-5-carboxylic acid). Microchimica Acta 183(1):361-368

117. Shang T, Wang P, Liu X, Jiang X, Hu Z, Lu X (2018) Facile synthesis of porous single-walled carbon nanotube for sensitive detection of 8-Hydroxy-2′-deoxyguanosine. Journal of Electroanalytical Chemistry 808:28-34

118. Wan C, Liu T, Wei S, Zhang S (2008) Electrochemical determination of 8-hydroxydeoxyguanosine using a carbon nanotube modified electrode. Russ J Electrochem 44(3):327-331

119. Zhang T-T, Zhao H-M, Fan X-F, Chen S, Quan X (2015) Electrochemiluminescence immunosensor for highly sensitive detection of 8-hydroxy-2′-deoxyguanosine based on carbon quantum dot coated Au/SiO2 core–shell nanoparticles. Talanta 131:379-385

120. Dhulkefl AJ, Atacan K, Bas SZ, Ozmen M (2020) An Ag–TiO 2–reduced graphene oxide hybrid film for electrochemical detection of 8-hydroxy-2′-deoxyguanosine as an oxidative DNA damage biomarker. Analytical Methods 12(4):499-506

121. Varodi C, Pogacean F, Coros M, Rosu M-C, Stefan-van Staden R-I, Gal E, Tudoran L-B, Pruneanu S, Mirel S (2019) Detection of 8-Hydroxy-2′-Deoxyguanosine Biomarker with a Screen-Printed Electrode Modified with Graphene. Sensors 19(19):4297

122. E Presnell C, Bhatti G, S Numan L, Lerche M, K Alkhateeb S, Ghalib M, Shammaa M, Kavdia M (2013) Computational insights into the role of glutathione in oxidative stress. Current neurovascular research 10(2):185-194

123. Mytilineou C, Kramer BC, Yabut JA (2002) Glutathione depletion and oxidative stress. Parkinsonism & related disorders 8(6):385-387

124. Bano D, Chandra S, Yadav PK, Singh VK, Hasan SH (2020) Off-on detection of glutathione based on the nitrogen, sulfur codoped carbon quantum dots@ MnO2 nano-composite in human lung cancer cells and blood serum. Journal of Photochemistry and Photobiology A: Chemistry:112558

125. Harfield JC, Batchelor-McAuley C, Compton RG (2012) Electrochemical determination of glutathione: a review. Analyst 137(10):2285-2296

126. Lee P, Ward K, Tschulik K, Chapman G, Compton R (2014) Electrochemical detection of glutathione using a poly (caffeic acid) nanocarbon composite modified electrode. Electroanalysis 26(2):366-373

127. Childs S, Haroune N, Williams L, Gronow M (2016) Determination of cellular glutathione: glutathione disulfide ratio in prostate cancer cells by high performance liquid chromatography with electrochemical detection. Journal of Chromatography A 1437:67-73

128. Lei P, Zhou Y, Zhu R, Liu Y, Dong C, Shuang S (2019) Facile synthesis of iron phthalocyanine functionalized N, B–doped reduced graphene oxide nanocomposites and sensitive electrochemical detection for glutathione. Sensors and Actuators B: Chemical 297:126756

129. Liu Q, Bao J, Yang M, Wang X, Lan S, Hou C, Wang Y, Fa H (2018) A core-shell MWCNT@ rGONR heterostructure modified glassy carbon electrode for ultrasensitive electrochemical detection of glutathione. Sensors and Actuators B: Chemical 274:433-440

130. Gao W, Liu Z, Qi L, Lai J, Kitte SA, Xu G (2016) Ultrasensitive glutathione detection based on lucigenin cathodic electrochemiluminescence in the presence of MnO2 nanosheets. Anal Chem 88(15):7654-7659

131. He H, Du J, Hu Y, Ru J, Lu X (2013) Detection of glutathione based on nickel hexacyanoferrate film modified Pt ultramicroelectrode by introducing cetyltrimethylammonium bromide and Au nanoparticles. Talanta 115:381-385

132. Rezaei B, Khosropour H, Ensafi AA, Hadadzadeh H, Farrokhpour H (2014) A differential pulse voltammetric sensor for determination of glutathione in real samples using a Trichloro (terpyridine) ruthenium (III)/Multiwall carbon nanotubes modified paste electrode. IEEE Sens J 15(1):483-490

133. Vinoth V, Wu JJ, Asiri AM, Anandan S (2017) Sonochemical synthesis of silver nanoparticles anchored reduced graphene oxide nanosheets for selective and sensitive detection of glutathione. Ultrason Sonochem 39:363-373

134. Ru J, Du J, Qin D-D, Huang B-M, Xue Z-H, Zhou X-B, Lu X-Q (2013) An electrochemical glutathione biosensor: Ubiquinone as a transducer. Talanta 110:15-20

135. Çubukçu M, Ertaş FN, Anık Ü (2013) Centri-voltammetric determination of glutathione. Microchimica Acta 180(1-2):93-100

136. Wahyuni WT, Rohaeti E, Sari DR (2018) Graphene Modified Screen Printed Carbon Electrode for Voltammetric Detection of Glutathione as Oxidative Stress Biomarker. E&ES 187(1):012078

137. Stojanović ZS, Đurović AD, Ashrafi AM, Koudelková Z, Zítka O, Richter L (2020) Highly sensitive simultaneous electrochemical determination of reduced and oxidized glutathione in urine samples using antimony trioxide modified carbon paste electrode. Sensors and Actuators B: Chemical:128141

138. Ma S, Yang Q, Zhang W, Xiao G, Wang M, Cheng L, Zhou X, Zhao M, Ji J, Zhang J (2020) Silver Nanoclusters and Carbon Dots Based Light-Addressable Sensors for Multichannel Detections of Dopamine and Glutathione and Its Applications in Probing of Parkinson's Diseases. Talanta:121290

139. Mazloum-Ardakani M, Tavakolian-Ardakani Z, Banitaba H (2020) Electrochemical determination of glutathione in hemolysed erythrocytes. Scientia Iranica

140. Rawat B, Mishra KK, Barman U, Arora L, Pal D, Paily RP (2020) Two-Dimensional MoS 2-Based Electrochemical Biosensor for Highly Selective Detection of Glutathione. IEEE Sens J 20(13):6937-6944

141. Fu X, Cate SA, Dominguez M, Osborn W, Özpolat T, Konkle BA, Chen J, López JA (2019) Cysteine disulfides (Cys-ss-X) as sensitive plasma biomarkers of oxidative stress. Scientific reports 9(1):1-9

142. Morris AA, Ko Y-A, Udeshi E, Jones DP, Butler J, Quyyumi A (2018) Novel Biomarkers of Oxidative Stress are Associated with Risk of Death and Hospitalization in Patients with Heart Failure. Journal of Cardiac Failure 24(8):S21

143. Madasamy T, Santschi C, Martin OJ (2015) A miniaturized electrochemical assay for homocysteine using screen-printed electrodes with cytochrome c anchored gold nanoparticles. Analyst 140(17):6071-6078

144. Shaidarova L, Ziganshina S, Tikhonova L, Budnikov G (2003) Electrocatalytic oxidation and flow-injection determination of sulfur-containing amino acids at graphite electrodes modified with a ruthenium hexacyanoferrate film. J Anal Chem 58(12):1144-1150

145. Mani V, Huang S-T, Devasenathipathy R, Yang TC (2016) Electropolymerization of cobalt tetraamino-phthalocyanine at reduced graphene oxide for electrochemical determination of cysteine and hydrazine. RSC advances 6(44):38463-38469

146. Yosypchuk B, Novotný L (2002) Cathodic stripping voltammetry of cysteine using silver and copper solid amalgam electrodes. Talanta 56(5):971-976

147. Ge S, Yan M, Lu J, Zhang M, Yu F, Yu J, Song X, Yu S (2012) Electrochemical biosensor based on graphene oxide–Au nanoclusters composites for l-cysteine analysis. Biosensors and Bioelectronics 31(1):49-54

148. Cao F, Dong Q, Li C, Kwak D, Huang Y, Song D, Lei Y (2018) Sensitive and Selective Electrochemical Determination of L- Cysteine Based on Cerium Oxide Nanofibers Modified Screen Printed Carbon Electrode. Electroanalysis 30(6):1133-1139

149. Bananezhad A, Karimi- Maleh H, Ganjali MR, Norouzi P (2018) MnO2- TiO2 Nanocomposite and 2- (3, 4- Dihydroxyphenethyl) Isoindoline- 1, 3- Dione as an Electrochemical Platform for the Concurrent Determination of Cysteine, Tryptophan and Uric Acid. Electroanalysis 30(8):1767-1773

150. Ensafi AA, Dadkhah-Tehrani S, Karimi-Maleh H (2011) A voltammetric sensor for the simultaneous determination of L-cysteine and tryptophan using a p-aminophenol-multiwall carbon nanotube paste electrode. Anal Sci 27(4):409-409

151. Dong Y, Pei L, Chu X, Zhang W, Zhang Q (2010) Electrochemical behavior of cysteine at a CuGeO3 nanowires modified glassy carbon electrode. Electrochim Acta 55(18):5135-5141

152. Hsiao Y-P, Su W-Y, Cheng J-R, Cheng S-H (2011) Electrochemical determination of cysteine based on conducting polymers/gold nanoparticles hybrid nanocomposites. Electrochim Acta 56(20):6887-6895

153. Lee PT, Thomson JE, Karina A, Salter C, Johnston C, Davies SG, Compton RG (2015) Selective electrochemical determination of cysteine with a cyclotricatechylene modified carbon electrode. Analyst 140(1):236-242

154. Nezamzadeh-Ejhieh A, Hashemi H-S (2012) Voltammetric determination of cysteine using carbon paste electrode modified with Co (II)-Y zeolite. Talanta 88:201-208

155. Yao J, Liu C, Liu L, Chen M, Yang M (2018) An Electrochemical Sensor for Sensitive Determination of L-cysteine and Its Electrochemical Kinetics on AgNPs/GQDs/GCE Composite Modified Electrode. J Electrochem Soc 165(13):B551

156. Wang Y, Wang W, Li G, Liu Q, Wei T, Li B, Jiang C, Sun Y (2016) Electrochemical detection of L-cysteine using a glassy carbon electrode modified with a two-dimensional composite prepared from platinum and Fe 3 O 4 nanoparticles on reduced graphene oxide. Microchimica Acta 183(12):3221-3228

157. Sonkar PK, Ganesan V, Rao V (2014) Electrocatalytic oxidation and determination of cysteine at oxovanadium (IV) salen coated electrodes. International Journal of Electrochemistry 2014

158. Maheshwari H, Vila N, Herzog G, Walcarius A (2020) Selective detection of cysteine at a mesoporous silica film electrode functionalized with ferrocene in the presence of glutathione. ChemElectroChem 7(9):2095-2101

159. Beitollahi H, Ganjali MR, Norouzi P, Movlaee K, Hosseinzadeh R, Tajik S (2020) A novel electrochemical sensor based on graphene nanosheets and ethyl 2-(4-ferrocenyl-[1, 2, 3] triazol-1-yl) acetate for electrocatalytic oxidation of cysteine and tyrosine. Measurement 152:107302

160. Peng J, Huang Q, Liu Y, Huang Y, Zhang C, Xiang G (2020) Photoelectrochemical detection of L- cysteine with a covalently grafted ZnTAPc- Gr- based probe. Electroanalysis

161. Luo S, Levine RL (2009) Methionine in proteins defends against oxidative stress. The FASEB Journal 23(2):464-472

162. Peng H, Deng H, Jian M, Liu A, Bai F, Lin X, Chen W (2017) Electrochemiluminescence sensor based on methionine-modified gold nanoclusters for highly sensitive determination of dopamine released by cells. Microchimica A

163. Gómez-Mingot M, Iniesta J, Montiel V, Kadara RO, Banks CE (2011) Direct oxidation of methionine at screen printed graphite macroelectrodes: towards rapid sensing platforms. Sensors and Actuators B: Chemical 155(2):831-836

164. Agüı L, Manso J, Yáñez-Sedeño P, Pingarrón J (2004) Colloidal-gold cysteamine-modified carbon paste electrodes as suitable electrode materials for the electrochemical determination of sulphur-containing compounds: application to the determination of methionine. Talanta 64(4):1041-1047

165. Sasikumar R, Ranganathan P, Chen S-M, Kavitha T, Lee S-Y, Chen T-W, Chang W-H (2017) Electrochemical determination of sulfur-containing amino acid on Screen-Printed Carbon Electrode modified with Graphene Oxide. Int J Electrochem Sci 12:4077-4085

166. Perevezentseva D, Skirdin K, Gorchakov E, Bimatov V (2016) Electrochemical activity of methionine at graphite electrode modified with gold nanoparticles. In: Key Eng Mater. Trans Tech Publ, pp 563-568

167. Odewunmi NA, Kawde A-N, Ibrahim M (2019) In-situ single-step electrochemical AgO modified graphite pencil electrode for trace determination of DL-methionine in human serum sample. Sensors and Actuators B: Chemical 281:765-773

168. Turunen M, Olsson J, Dallner G (2004) Metabolism and function of coenzyme Q. Biochimica et Biophysica Acta (BBA)-Biomembranes 1660(1-2):171-199

169. James AM, Smith RA, Murphy MP (2004) Antioxidant and prooxidant properties of mitochondrial Coenzyme Q. Arch Biochem Biophys 423(1):47-56

170. Acosta MJ, Fonseca LV, Desbats MA, Cerqua C, Zordan R, Trevisson E, Salviati L (2016) Coenzyme Q biosynthesis in health and disease. Biochimica et Biophysica Acta (BBA)-Bioenergetics 1857(8):1079-1085

171. Ó Conghaile P, Arrigan DW (2022) Ubiquinone electrochemistry in analysis and sensing. Electrochemical Science Advances:e2100214

172. Barsan MM, Diculescu VC (2019) New electrochemical sensor based on CoQ10 and cyclodextrin complexes for the detection of oxidative stress initiators. Electrochim Acta 302:441-448

173. Li D, Deng W, Xu H, Sun Y, Wang Y, Chen S, Ding X (2016) Electrochemical investigation of coenzyme Q10 on silver electrode in ethanol aqueous solution and its determination using differential pulse voltammetry. Journal of laboratory automation 21(4):579-589

174. Charoenkitamorn K, Chaiyo S, Chailapakul O, Siangproh W (2018) Low-cost and disposable sensors for the simultaneous determination of coenzyme Q10 and α-lipoic acid using manganese (IV) oxide-modified screen-printed graphene electrodes. Analytica Chimica Acta 1004:22-31

175. Schou-Pedersen AMV, Schemeth D, Lykkesfeldt J (2019) Determination of reduced and oxidized coenzyme Q10 in canine plasma and heart tissue by HPLC-ECD: comparison with LC-MS/MS quantification. Antioxidants 8(8):253

176. Seifar F, Khalili M, Khaledyan H, Amiri Moghadam S, Izadi A, Azimi A, Shakouri SK (2019) α-Lipoic acid, functional fatty acid, as a novel therapeutic alternative for central nervous system diseases: A review. Nutritional neuroscience 22(5):306-316

177. Xiang W, Wang L, Cheng S, Zhou Y, Ma L (2019) Protective Effects of α-Lipoic Acid on Vascular Oxidative Stress in Rats with Hyperuricemia. Current Medical Science 39(6):920-928

178. Ziyatdinova G, Budnikov G, Pogorel'tsev V (2004) Electrochemical determination of lipoic acid. J Anal Chem 59(3):288-290

179. Miranda M, Del Rio R, Del Valle M, Faundez M, Armijo F (2012) Use of fluorine-doped tin oxide electrodes for lipoic acid determination in dietary supplements. Journal of Electroanalytical Chemistry 668:1-6

180. Stankovic DM, Mehmeti E, Kalcher K (2016) Development of sensitive analytical approach for the quantification of α-lipoic acid using boron doped diamond electrode. Anal Sci 32(8):847-851

181. Ferreira APM, dos Santos Pereira LN, da Silva IS, Tanaka SM, Tanaka AA, Angnes L (2014) Determination of α- Lipoic acid on a Pyrolytic Graphite Electrode Modified with Cobalt Phthalocyanine. Electroanalysis 26(10):2138-2144

182. Sasikumar R, Ranganathan P, Chen S-M, Rwei S-P (2018) f-MWCNTs-PIN/Ti2O3 nanocomposite: Preparation, characterization and nanomolar detection of α-Lipoic acid in vegetables. Sensors and Actuators B: Chemical 255:217-225

183. Ziyatdinova G, Antonova T, Vorobev V, Osin Y, Budnikov H (2019) Selective voltammetric determination of α-lipoic acid on the electrode modified with SnO 2 nanoparticles and cetyltriphenylphosphonium bromide. Monatshefte für Chemie-Chemical Monthly 150(3):401-410

184. Skorupa A, Michalkiewicz S (2020) Voltammetric Determination of α-Lipoic Acid using Carbon Fiber Microelectrode in Acetic Acid–Acetonitrile Solutions. Int J Electrochem Sci 15:1581-1594

185. Vítek L (2020) Bilirubin as a signaling molecule. Medicinal Research Reviews

186. Yao Q, Jiang X, Huang Z-W, Lan Q-H, Wang L-F, Chen R, Li X-Z, Kou L, Xu H-L, Zhao Y-Z (2019) Bilirubin improves the quality and function of hypothermic preserved islets by its antioxidative and anti-inflammatory effect. Transplantation 103(12):2486-2496

187. Ziberna L, Martelanc M, Franko M, Passamonti S (2016) Bilirubin is an endogenous antioxidant in human vascular endothelial cells. Scientific reports 6:29240

188. Fevery J (2008) Bilirubin in clinical practice: a review. Liver International 28(5):592-605

189. Kannan P, Chen H, Lee VT-W, Kim D-H (2011) Highly sensitive amperometric detection of bilirubin using enzyme and gold nanoparticles on sol–gel film modified electrode. Talanta 86:400-407

190. Manikandan PN, Imran H, Dharuman V (2019) Self- powered polymer–metal oxide hybrid solar cell for non- enzymatic potentiometric sensing of bilirubin. Medical Devices & Sensors 2(2):e10031

191. Akhoundian M, Alizadeh T, Pan G (2020) Fabrication of the Enzyme- less Voltammetric Bilirubin Sensor Based on Sol- gel Imprinted Polymer. Electroanalysis 32(3):479-488

192. Sivalingam T, Devasena T, Dey N, Maheswari U (2019) Curcumin-Loaded Chitosan Sensing System for Electrochemical Detection of Bilirubin. Sensor Letters 17(3):228-236

193. Zheng Z, Feng Q, Zhu M, Shang J, Li M, Li C, Kou L, Zheng J, Wang C (2019) Electrochemical sensor for the discrimination of bilirubin in real human blood based on Au nanoparticles/tetrathiafulvalene–carboxylate functionalized reduced graphene oxide 0D-2D heterojunction. Analytica chimica acta 1072:46-53

194. Bell JG, Mousavi MP, Abd El-Rahman MK, Tan EK, Homer-Vanniasinkam S, Whitesides GM (2019) based potentiometric sensing of free bilirubin in blood serum. Biosensors and Bioelectronics 126:115-121

195. Taurino I, Van Hoof V, Magrez A, Forró L, De Micheli G, Carrara S (2014) Efficient voltammetric discrimination of free bilirubin from uric acid and ascorbic acid by a CVD nanographite-based microelectrode. Talanta 130:423-426

196. Narang J, Chauhan N, Mathur A, Chaturvedi V, Pundir C (2015) A third generation bilirubin sensor development by using gold nanomaterial as an immobilization matrix for signal amplification. Adv Mater Lett 6:1012-1017

197. Thangamuthu M, Gabriel WE, Santschi C, Martin OJ (2018) Electrochemical sensor for bilirubin detection using screen printed electrodes functionalized with carbon nanotubes and graphene. Sensors 18(3):800

198. Dehghani H, Khoramnejadian S, Mahboubi M, Sasani M, Ghobadzadeh S, Haghighi SM, Negahdary M (2016) Bilirubin biosensing by using of catalase and ZnS nanoparticles as modifier. Int J Electrochem Sci 11:2029-2045

199. Zhang C, Bai W, Qin T, Yang Z (2018) Fabrication of Red Mud/Molecularly Imprinted Polypyrrole-Modified Electrode for the Piezoelectric Sensing of Bilirubin. IEEE Sens J 19(4):1280-1284

200. Rahman MM, Ahmed J, Asiri AM (2019) Selective bilirubin sensor fabrication based on doped IAO nanorods for environmental remediation. New J Chem 43(48):19298-19307